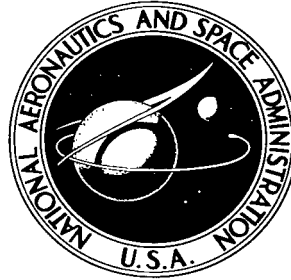


NASA TECHNICAL NOTE



NASA TN D-3571

NASA TN D-3571

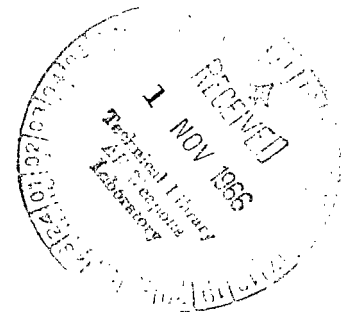
c. 1

LOAN COPY: RET  
AFWL (WLI)  
KIRTLAND AFB,



# PROJECT FIRE PHOTOGRAPHIC SUMMARY AND RECORD OF REENTRY PHENOMENA AT HYPERBOLIC VELOCITIES

*by Charles W. McKee*  
*Langley Research Center*  
*Langley Station, Hampton, Va.*





PROJECT FIRE PHOTOGRAPHIC SUMMARY AND RECORD OF  
REENTRY PHENOMENA AT HYPERBOLIC VELOCITIES

By Charles W. McKee

Langley Research Center  
Langley Station, Hampton, Va.

Technical Film Supplement L-893 available on request.

NATIONAL AERONAUTICS AND SPACE ADMINISTRATION

---

For sale by the Clearinghouse for Federal Scientific and Technical Information  
Springfield, Virginia 22151 - Price \$2.50

# PROJECT FIRE PHOTOGRAPHIC SUMMARY AND RECORD OF REENTRY PHENOMENA AT HYPERBOLIC VELOCITIES

By Charles W. McKee  
Langley Research Center

## SUMMARY

Project Fire was undertaken by the National Aeronautics and Space Administration to measure the total and radiative heating experienced by a blunt body reentering the earth's atmosphere at 11 300 meters per second. This report presents a photographic record of the Fire II spacecraft during its reentry. The photographs were clear enough to establish the times of major events, and they show that adequate separation was maintained between the reentry package and the spent Antares. This report also identifies operational problems encountered in spacecraft reentry at hyperbolic velocities and presents the solutions satisfactorily employed.

## INTRODUCTION

The purpose of Project Fire was to gather in-flight measurements of the reentry heating environment which would be encountered by spacecraft returning from the moon or the near planets. The actual in-flight measurements from a large-scale vehicle were needed to establish a bench mark from which further heating studies and calculations could proceed. The project consisted of two flights with reentries at 11 560 and 11 350 meters per second. The spacecraft were launched from Kennedy Space Center, Florida, down the Eastern Test Range with reentry occurring in the Ascension Island area. The first spacecraft, Fire I, was launched April 14, 1964 at 21 hours 42 minutes 25.536 seconds Greenwich mean time (GMT). The second spacecraft, Fire II, was launched May 22, 1965 at 21 hours 54 minutes 59.703 seconds GMT. Only meager optical coverage was obtained for Fire I because of cloud cover in the reentry area. For Fire II, excellent viewing conditions permitted extensive optical coverage from both ground and airborne instrumentation.

Sequential photographs of the hyperbolic-velocity reentry phenomena and some representative samples of optical-signature data as reduced by the Eastern Test Range are presented herein. This report shows the utility of optical-signature-data gathering and recognizes its value as a tool for both experimental analysis and failure analysis.

Also, motion-picture supplement L-893 has been prepared and is available on loan. A request card and a description of the film are included at the back of this document.

## DESCRIPTION OF EXPERIMENT

In order to gather the desired heating data during atmospheric reentry at speeds near 11 300 meters per second, a highly instrumented reentry package having a diameter of 67.2 centimeters and weighing 86.54 kilograms was accelerated back into the earth's atmosphere from a ballistic trajectory by a velocity package. The velocity package utilizing an Antares II-A5 solid-propellant rocket motor and its own guidance and control system was designed to provide spin stabilization, the required thrust, and attitude control to place the reentry package in a planned reentry flight path at the desired velocity. This spacecraft combination composed of the reentry package and the velocity package was lifted into a ballistic trajectory down the Eastern Test Range by an Atlas D launch vehicle (see fig. 1). A more detailed description of the space-vehicle hardware may be found in reference 1.

The Project Fire reentry package was designed to provide heating measurements during the peak heating period to be encountered during atmospheric reentry of a blunt body at 11 300 meters per second. The measurements of total heating and radiative heating were made at selected periods during the reentry. The reentry package was designed to obtain accurate radiation measurements in a clean environment with a minimum of ablation products present. Total heating measurements were made from the forebody calorimeters. As it is impossible to fabricate a single calorimeter that will survive the heat of reentry, the forebody of the reentry package was constructed of six layers. The first, third, and fifth layers were made of beryllium and were instrumented with thermocouples to provide measurements of temperature time histories. A detailed explanation of the beryllium calorimeter layers is included in reference 2. The second, fourth, and sixth layers were phenolic asbestos ablation shields to protect the beryllium shields until the proper experiment time, at which time the ablation shields were ejected. The reentry package was additionally instrumented to obtain measurements of angular rates and accelerations, afterbody pressure, and voltage standing-wave ratio. All these data were transmitted to ground, ship, and airborne telemetry stations in the Ascension Island area by a dual telemetry transmitting system contained in the reentry package.

Figure 2 presents photographs of the exterior and interior of the reentry package and a drawing showing the arrangement of the forebody calorimeters and ablation shields. The afterbody structure was primarily fiber glass with a phenolic asbestos cover which was coated with silicone elastomer containing silica microballoons. The afterbody was a 66° cone attached to the forebody by an aluminum flange. The beacon and telemetry

antennas were coated with teflon. The reentry package was held in place for launch atop the Antares motor by the fiber-glass adapter section shown in figure 3.

### PHYSICAL CONFIGURATION

A knowledge of the physical configuration of the reentry complex and the proximity of the components to each other during reentry is helpful during evaluation of the photographic record. Figure 4 identifies the major components of the reentering complex and lists their physical characteristics. As an aid in a spectrographic analysis of the reentry phenomena, samples of the spacecraft materials were analyzed by the Chemical Laboratory of the Eastern Test Range (ref. 3). This analysis was made to facilitate the identification of materials by means of the spectral radiation emitted during the atmospheric reentry. The results are shown in table I, where the three classifications – major, minor, and trace – indicate the percentage of element emitted.

TABLE I.- SPECTROGRAPHIC ANALYSIS OF SPACECRAFT MATERIALS\*

Element	Beryllium calorimeter	Calorimeter wire	Phenolic asbestos	Silicone elastomer	Antares motor case - resinous	Antares motor case - nonresinous	High-heat silicone paint	Ejection-spring chrome-vanadium steel
Pb	----	----	----	----	----	----	Trace	----
Ag	----	----	Trace	----	----	----	----	----
Na	----	----	----	Minor	----	Major	----	----
Ca	----	----	----	Trace	Trace	Major	Trace	----
Ti	----	----	----	Trace	Trace	Major	Minor	----
Zn	----	----	----	----	Minor	Trace	Trace	----
Cr	----	----	----	----	Minor	Minor	Trace	Major
Bi	----	----	----	----	----	Trace	----	----
Sr	----	----	----	----	----	Trace	----	----
Ga	----	----	----	----	----	----	Trace	----
Rh	----	----	----	----	----	----	Trace	----
Hg	----	----	----	----	----	----	Trace	----
Mo	----	----	----	----	----	----	----	Minor
V	----	----	----	----	----	----	----	Minor
Mn	----	Major	----	----	Minor	Trace	Minor	Minor
Ni	Trace	Major	Minor	----	Minor	----	----	Minor
Si	Trace	Minor	Major	Major	Major	Major	Major	----
Mg	Minor	Trace	Major	Trace	Major	Minor	Trace	----
Cu	Trace	Trace	----	----	Trace	Trace	Trace	Minor
Be	Major	----	----	----	----	----	----	----
Fe	Minor	----	Minor	Trace	Minor	Minor	Minor	Major
Al	Trace	----	Minor	Trace	Trace	Major	Major	----
B	----	----	Trace	Minor	Trace	Major	Trace	----

\*Classifications:

Major - more than 75 percent.

Minor - between 1.0 and 5.0 percent.

Trace - less than 1.0 percent.

## INSTRUMENTATION SUPPORT

The Eastern Test Range provided the necessary support in the reentry area to insure that telemetry recording, ballistic camera coverage, adequate optical and radar tracking, and limited radiometric and spectral coverage would be available. The instrumentation support provided by the Eastern Test Range for the two Project Fire launches is given in table II.

**TABLE II.- EASTERN TEST RANGE INSTRUMENTATION SUPPORT  
FOR PROJECT FIRE LAUNCHES**

Instrumentation	Support for -
Launch area radar tracking	Fire I and Fire II 
Launch area metric optics	
Launch area telemetry <sup>a</sup>	
Midrange radar tracking	
Midrange telemetry	
Terminal area radar tracking	
Terminal area metric optics	
Terminal area infrared tracking	
Terminal area multiple target tracking	
Terminal area spectral recording	
Terminal area radiometric recording	Fire II <sup>b</sup>
Terminal area telemetry	Fire II <sup>c</sup>
Terminal area tracking and telemetry ship	Fire I and Fire II 
Terminal area telemetry aircraft	

<sup>a</sup>Primary spacecraft coverage by Kennedy Space Center with Eastern Test Range used as a backup.

<sup>b</sup>Coverage for Fire I provided by ZEUS Project Office, U.S. Army Materiel Command.

<sup>c</sup>The American Mariner tracking ship was committed to support Fire I, but because of an excessive amount of time on station and the low fuel supply the ship was withdrawn prior to the launch.

During the countdown for the Project Fire launches, the Eastern Test Range telemetry aircraft stationed in the reentry area performed the role of weather reconnaissance. For the Fire I launch the reconnaissance indicated that a clearing condition was moving toward the reentry area and provided the only assurance of acceptable weather for launch. For the Fire II launch the reconnaissance confirmed a clearing condition in the reentry area better than had been forecast.

In order to supplement the Eastern Test Range capability and to provide for additional data collection, Langley Research Center supplied four 920-millimeter fixed spectral cameras with 300-line/millimeter gratings and contracted for the installation and operation of a tracking telespectrograph (a Cassegrain optical instrument with 91.4-centimeter aperture and 7.3-meter focal length) on Ascension Island. Because of a combination of inaccuracies in translation of tracking signal and errors in judgment by the operator, the tracking telespectrograph failed to record useful data during the reentry period. Goddard Space Flight Center (GSFC) also supplemented the Eastern Test Range capability. In the terminal area GSFC provided, for Fire I, an optically equipped aircraft and, for Fire II, two optically equipped aircraft, one of which also had a telemetry backup capability. The Kennedy Space Center provided documentary photography coverage for the Project Fire operations.

### SEQUENCE OF EVENTS

The specific times of occurrence of the major events for both Fire I and Fire II are listed in table III. Following launch of the space vehicle, ejection of the protective shroud, and separation of the spacecraft from the launch vehicle, the spacecraft entered a coast phase during which the velocity-package guidance system reoriented the spacecraft to a reentry attitude of  $-15^{\circ}$  to the horizon. After coast through apogee the velocity package was programmed to deactivate its guidance system, ignite the spin rockets to spin stabilize the reentry package, separate the velocity-package shell, and ignite the Antares solid-propellant motor. Following burnout of the Antares motor, the reentry package was separated from the spent motor case and the small rocket motors on the reentry-package adapter were ignited. A tumble rocket motor was used on the Fire I reentry-package adapter; a despin rocket motor and a retrorocket motor were used on the Fire II adapter. These motors were positioned to despin the spent Antares motor, cause it to tumble, and translate it from the reentry-package flight path. During the Fire I reentry the separation distance between the reentry package and the spent Antares became so small that the flow field from the spent Antares induced some undesirable body motions in the reentry package (ref. 1). Mounted between the Antares motor and the reentry-package adapter on Fire II was a large asymmetrical drag plate to increase the

aerodynamic drag of the spent motor case and insure adequate separation between the reentry package and the spent Antares.

For the Fire II flight it was decided to move the spacecraft reentry track 18 kilometers closer to Ascension Island and to move the impact point uprange 150 kilometers. This trajectory change provided a much better opportunity for obtaining good optical coverage and also placed the reentry-package telemetry antenna pattern in its best relationship to the ground station during the delayed playback period. The Fire I and Fire II ground tracks in relation to Ascension Island are illustrated in figure 5.

TABLE III.- SEQUENCE OF EVENTS FOR PROJECT FIRE SPACECRAFT

Flight event	Elapsed time from launch, sec	
	Fire I	Fire II
Enable velocity-package ignition interlock (signal transmission)	128.0	126.75
Start velocity-package timer (signal transmission)	295.38	294.386
Jettison velocity-package shroud (signal transmission)	298.0	295.284
Uncage velocity-package gyros (signal transmission)	306.0	304.59
Separate spacecraft (onboard programmer)	311.5	308.73
Start velocity-package pitch program	319.88	334.874
End velocity-package pitch program	421.39	435.03
Start reentry-package separation timers	1567.57	1538.0
Fire spin rockets	1574.31	1545.0
Ignite Antares II-A5 delay squib	1574.31	1545.0
Separate velocity-package shell	1577.32	1548.0
Ignite Antares II-A5	1580.31	1551.34
Burnout of Antares II-A5 (main thrust termination)	1613.13	1583.0
Separate reentry package	1640.46	1610.43
Ignite tumble motors	1646.46	1616.43
Arrive at 121 920-meter altitude	1647.36	1617.74
Begin telemetry blackout	1653.9	1624.7
Start reentry timer (10.4g deceleration)	1666.6	1639.11
Eject first heat shield (pyrofuze link signal)	1669.6	1642.12
Eject second heat shield (pyrofuze link signal)	1676.6	1647.53
End telemetry blackout	1686.8	1655.1
Disable record and erase head	1689.0	1661.48
Activate failover switch	1851.5	1696.11
Reentry-package impact	1965.7	1934.3

## RESULTS AND DISCUSSION

### Fire I Reentry

The photographic coverage obtained for the Fire I reentry was severely hampered by a cloudy sky condition and by the fact that the reentry portion of the flight presented a far more difficult tracking target than the operators of the photographic equipment had envisioned. (See fig. 6.) No previous tracking of an object traveling at the velocity planned for the Project Fire reentry package had been attempted by the Eastern Test Range, and the short data period of only 40 seconds permitted little opportunity to correct for an error in judgment or tracking rate. Also, the tracking of the reentry package was hindered by the fact that following closely behind the reentry package was a far brighter and more spectacular object, the spent Antares motor. The difficulty in acquiring and maintaining track of the reentry package was recognized prior to the flight, and a program of instructions and training for operators of optical and electronic tracking equipment was conducted. However, the lack of experience in tracking objects at the Fire reentry speed together with the poor visibility resulted in a poor photographic record of Fire I reentry. The value of the photographic record was emphasized during subsequent investigations conducted to determine the cause of some unexpected body motions experienced by the reentry package (ref. 1).

The Avco-Everett Research Laboratory working under an Air Force contract was successful in obtaining some good coverage of the Fire I reentry from airborne instrumentation. The data obtained are presented in reference 4.

### Fire II Reentry

The photographic coverage of the Fire II reentry was excellent. The engineering sequential and documentary coverage of the reentry permitted positive verification of important events and showed that adequate separation was maintained between the reentry package and the other spacecraft components.

Open-shutter camera coverage.- Figure 7 is a montage of the Fire II reentry as recorded by three open-shutter streak cameras located on Ascension Island. These K-37 cameras of 300-millimeter focal length used 038.01 high-speed panchromatic emulsion. Figure 8 is an open-shutter photograph of the entire reentry taken from an NASA airplane. This single photograph covers the time from first acquisition of the reentering spacecraft (right end of upper trace) at approximately 1633.324 seconds until final burnup of the last launch vehicle part (left end of lower trace) at approximately 1698.423 seconds. This photograph of 65 seconds duration was made with a minimum of photographic distortion, as can be appreciated by comparing it with a montage made from the ground-based still cameras. The airplane wing (see lower right corner of figure)

was illuminated by available light from the reentry phenomena. The upper trace is the reentry package and the spent Antares motor case following the same trajectory. The small trace located slightly above the large lower trace is the velocity-package shell which was ejected after spinup and before the Antares ignition. The large lower trace is the launch vehicle, and the point of residual fuel explosion and subsequent breakup of the vehicle can be seen.

Engineering sequential coverage.- Sixteen selected sequences of the Fire II reentry photography are reproduced in appendix A and are referred to throughout this report. These sequences were recorded by the Intermediate Focal Length Optical Tracker (IFLOT) camera system located on Ascension Island. Figure 9 shows the Ascension Island instrumentation deployment. The Target Tracking Radar (TTR) is a C-band radar unit for skin tracking of multiple targets; the Mod. II is an S-band automatic tracking radar unit; the FPS-16 and the TPQ-18 are C-band radar units; and the TLM-18 is a high-gain telemetry receiving antenna. The sequences reproduced in the appendix were selected to provide a representative record of critical events and a verification of adequate separation between the reentry package and the spent Antares. To assist the reader in an interpretation of these photographs, tables of reentry-package velocity, slant range from the observation point, altitude, and time of exposure of each are also provided in the appendix (tables A-I and A-II).

Engineering sequential photography of the quality obtained during Fire II is an invaluable aid for verification of events, separation studies, wake studies, and failure analysis. Table IV lists the reentry events for Fire II which can be verified by existing photographs together with telemetry data.

TABLE IV.- FIRE II REENTRY EVENTS

Event	Time from launch, sec	Photographic record	Telemetry data
Tumble-motor ignition	1616.43	Figure 7	No
First-beryllium-calorimeter melt	1640	Sequence 7A	Yes
First-ablation-shield ejection	1642.12	Sequence 8	Yes
Second-beryllium-calorimeter melt	1645.5	Sequence 11	Yes
Second-ablation-shield ejection	1647.53	Sequence 14	Yes

Wake studies.- Wake studies were conducted to determine the size of the visible wake and gaslight image as recorded by the IFLOT camera system on Ascension Island. Measurements of both the width and the length of the visible pattern during the reentry

period were made from 70-millimeter black and white film. Figure 10 presents results of these studies for both the spent velocity package and the reentry package in relation to time. The possibility of optical halation effects or overexposure of the film was not considered when the wake measurements were made. Photographs taken with different camera systems and from different vantage points recorded wakes of comparable size. The tumbling motion of the spent Antares motor case and the adapter section caused the visible wake to fluctuate over wide ranges of length and width during the reentry. (See fig. 10(a).) The length of the visible wake fluctuated between 600 meters and 2100 meters as the spent velocity package penetrated the earth's atmosphere from an altitude of 75 kilometers to an altitude of 60 kilometers.

A comparison between the reentry-package wake lengths, as recorded on the color film and the black and white film at the same instant, reveals an interesting difference. At 1642.522 seconds the measured wake length from the color film is about 392 meters while the measured wake length from the black and white film (sequence 8C) is about 700 meters.

The difference in recorded image size is attributed to the different film emulsion and to the sensitivity of the film to the light source. Other comparisons are made at 1645.855 seconds and 1646.888 seconds. At 1645.855 seconds the color image of the wake is about 590 meters in length and the black and white image (sequence 12B) is about 766 meters. At 1646.888 seconds the length of the color image is about 492 meters and the length of the black and white image (sequence 13B) is about 656 meters.

Another interesting observation, made after the experiment period, is the presence of a long (about 700 to 1200 m) thin wake behind the reentry package at altitudes and velocities where ablation from the forebody heat shield is not present. A possible factor contributing to this wake is outgassing of the afterbody heat-protection material.

Optical signature data.- Additional data collected during the reentry in the form of spectrograms and photometric recordings were compiled and reduced by the Eastern Test Range Signature Processing. These reduced signature data have been analyzed primarily for diagnostic purposes. The reduced data are contained in reference 3. Caution should be exercised when using this reference. The time and trajectory differ from the time and trajectory used herein. In reference 3 the time is given to the nearest whole second and the trajectory information is derived from radar skin-track information for the spent Antares components rather than for the reentry package. Figure 11 lists the instrumentation and shows the times of coverage for signature data reduced by the Eastern Test Range. Samples of the spectrographs and samples of the type of reduction performed by the Eastern Test Range in support of Project Fire are presented in figures 12 and 13, respectively.

Analysis of separation distance between reentry package and spent Antares.- For the Fire II operation a special effort was made to prevent a recurrence of the undesirable body motion experienced by the Fire I reentry package (ref. 1). In an effort to insure adequate separation between the reentry package and the spent Antares case, an additional small rocket motor was utilized together with a drag plate, as shown in figure 3. A six-degree-of-freedom analysis predicted a separation distance which would increase from 38 meters at 1621.74 seconds to 2743 meters at 1642.74 seconds. In order to determine the effectiveness of the separation system, engineering sequential photography was used to calculate the longitudinal separation distance achieved during the Fire II reentry. The results show that the separation distance was larger than had been predicted (see fig. 14).

The photographic record of reentry also emphasized a potential source of concern for future reentry operations in which collision or near collision of bodies must be avoided. Large components or assemblies with a high ballistic number following behind reentering spacecraft must be designed to maintain structural integrity until they have been sufficiently decelerated or laterally displaced to avoid collision.

Analysis of visual observations from Ascension Island.- In an effort to gather the maximum amount of valid information on the hyperbolic-velocity reentry phenomenon and to eliminate the possibility of error due to faulty memory in reconstructing events at a later time, tape recorders were utilized by observers of the Fire II reentry. Three observers stationed at different sites on Ascension Island recorded their observations during the visible portion of the reentry. The three observers were in general agreement on colors observed, sequence of events, and the apparent velocity of the reentering complex. From their comments it is apparent that each of the observers witnessed the ignition of the tumble rockets on the spent Antares. Following the tumble rocket firing there were a few seconds during which the reentry was not visible. When the reentry again became visible, it appeared as a single point of blue-white light. This single point rapidly divided into two separate light sources, with the reentry package in front appearing to accelerate away from the spent Antares. The blue-white light changed to a yellow-orange appearance and, during the periods of beryllium melt, red was noticeable. As the spent Antares began to break up and burn, combinations of green, orange, and red appeared. The record of visual observations agrees with colors recorded on the color film of reentry.

Description of reentry.- Following is a description of the reentry as recorded by the IFLOT camera system utilizing both black and white film and color film. The sequences of black and white photographs referred to are reproduced in the appendix, and a color motion-picture film supplement (film serial L-893) is available on loan. The IFLOT camera system on Ascension Island recorded the Fire II reentry beginning at 22 hours 22 minutes 13.027 seconds GMT or 1633.324 seconds elapsed time from launch.

The IFLOT was successful in acquiring track of the reentry package early in its reentry and maintained track during the greater portion of the reentry period. At first visible acquisition, the reentering spacecraft (reentry package, spent Antares, and adapter) appeared as a single point source of blue-white light similar to a star of the sixth magnitude. This light rapidly became more intense and the reentry package and spent Antares were soon distinguishable as two separate light sources, with the spent Antares being the brighter of the two (sequence 1). Both light sources presented a changing pattern which was alternately bright and dim, the light sources becoming more brilliant with each alternation (sequences 2, 3, and 4). During this period from first acquisition until 1637.2 seconds, the blue-white light is changing to an intense yellow, with shades of red and green becoming visible in the trailing Antares and adapter portion. After 1638.4 seconds and until 1640.456 seconds, the Antares motor and the adapter show signs of severe breakup, with burning components displaying yellow, orange, white, blue, and green shades. During this time the reentry package has changed from a blue-white to a yellow-orange shade (sequences 5 to 7). During the early stages of Antares and adapter breakup, those components with a higher ballistic coefficient  $W/C_D A$  (where  $W$  is the component weight,  $C_D$  is the drag coefficient, and  $A$  is the cross-sectional area) are not being decelerated as rapidly as the larger mass of the Antares. Several such components are the despin rocket motor, the retrorocket motor, the Antares nozzle, the drag-plate counterbalance, and the battery. Track of the reentry package was lost by the IFLOT camera momentarily at 1639.687 seconds. It was at this time that the disintegrating Antares motor case and the adapter were most brilliant (sequence 7). Between 1640.1 and 1640.2 seconds a red trail which is the melting first beryllium calorimeter from the reentry package appears in front of the Antares, but the reentry package itself is out of the field of view to the left. When the reentry package comes into the field of view, it appears as a brilliant orange mass with a red wake streaming behind. The melting beryllium wake attains a visible length in excess of 750 meters. Following the beryllium melt it is possible to observe ejection of the first phenolic asbestos ablation shield and its subsequent burnup. The many pieces of the ejected ablation shield burn a bright yellow-orange for approximately 1 second (sequences 8 and 9). For a short period following ablation-shield ejection, the reentry package appears as a pale yellow light with no apparent melting or ablation present. The reentry package then begins to show effects of outgassing and ablation from the afterbody material, followed by increased heating of the calorimeter. This heating causes the reentry package to turn from yellow to a progressively brighter orange (sequences 10 and 11), and shortly thereafter the melting of the second beryllium calorimeter is identified by an intense red wake which attains a length in excess of 750 meters (sequences 12, 13, and 14). Following the second calorimeter melt the second ablation shield is ejected. The ejected pieces of the second ablation shield do not burn as brightly as did those of the first shield. The pieces give the appearance of cooling after ejection rather than of being completely consumed (sequence 15).

The ablation from the third beryllium calorimeter is less intense than that from either the first or second, because of a much lower velocity. Shortly after ejection of the second ablation shield, the distance from the camera together with the low elevation angle result in a restricted view of the reentry phenomena (sequence 16). A long thin wake from the reentry package is still visible for approximately 5 seconds but is not of sufficient intensity for good reproduction.

#### CONCLUDING REMARKS

Two Project Fire flights were conducted to collect the data necessary for a thorough analysis of the reentry heating phenomena. Data collected in the form of telemetric, spectrographic, and radiometric measurements, radar tracks, movie film, and streak-camera, chopped-camera, and engineering sequential photographs contribute to the establishment of a more accurate and current standard for predicting the heating environment which future spacecraft will encounter during reentry. A photographic record of the Fire II spacecraft reentry into the earth's atmosphere at hyperbolic velocities demonstrated the utility of optical data. The sequential photographs provided a verification of major flight events and showed that adequate separation was maintained between the reentry package and the spent Antares.

Langley Research Center,  
National Aeronautics and Space Administration,  
Langley Station, Hampton, Va., July 6, 1966.

## APPENDIX A

### ENGINEERING SEQUENTIAL PHOTOGRAPHY OF FIRE II REENTRY

Sixteen selected sequences of the Fire II reentry are presented. These sequences depict events in the following order: early gaslight of the reentry package and the spent Antares; increasing separation between the reentry package and the spent Antares; tumble, breakup, and burn of the spent Antares motor case and components; melt of the first beryllium calorimeter; jettison and burn of the first phenolic asbestos ablation shield; melt of the second beryllium calorimeter; jettison and burn of the second phenolic asbestos ablation shield; and afterbody ablation during the third data period. These events are also recorded in color on a film supplement.

The sequences shown herein were taken from the Intermediate Focal Length Optical Tracker (IFLOT) located on Cat Hill on Ascension Island and operated by the Eastern Test Range. The IFLOT equipment consisted of a power-driven tracking mount with a 70-millimeter photosonics camera having a 203-centimeter focal length lens. Tri-X film was used and was exposed at 30 frames per second. Table A-I lists velocity, slant range from the camera, and altitude of the reentry package during the reentry period. Table A-II lists the time of exposure of the sequential photographs in both Greenwich mean time and elapsed time from launch.

APPENDIX A

TABLE A-I.- VELOCITY, SLANT RANGE, AND ALTITUDE IN RELATION TO  
ELAPSED TIME OF THE FIRE II REENTRY PACKAGE  
AS VIEWED BY THE IFLOT CAMERA SYSTEM  
ON ASCENSION ISLAND

Elapsed time, sec	Velocity, m/sec	Slant range, m	Altitude, m
1634	11 357	155 608	76 424
1634.5	11 349	151 659	75 072
1635	11 340	147 825	73 724
1635.5	11 328	144 115	72 380
1636	11 314	140 539	71 040
1636.5	11 296	137 106	69 705
1637	11 275	133 830	68 375
1637.5	11 250	130 719	67 051
1638	11 220	127 788	65 732
1638.5	11 186	125 048	64 420
1639	11 144	122 509	63 115
1639.5	11 096	120 185	61 818
1640	11 039	118 085	60 530
1640.5	10 973	116 220	59 251
1641	10 897	114 598	57 983
1641.5	10 811	113 225	56 726
1642	10 713	112 106	55 483
1642.5	10 602	111 242	54 254
1643	10 478	110 634	53 041
1643.5	10 340	110 275	51 845
1644	10 186	110 161	50 667
1644.5	10 017	110 281	49 510
1645	9 830	110 623	48 375
1645.5	9 626	111 171	47 264
1646	9 406	111 908	46 179
1646.5	9 161	112 815	45 121
1647	8 895	113 871	44 093
1647.5	8 609	115 053	43 098
1648	8 303	116 340	42 137
1648.5	7 975	117 708	41 213
1649	7 631	119 134	40 327
1649.5	7 275	120 597	39 481
1650	6 913	122 079	38 676

APPENDIX A

TABLE A-II.- TIME OF EXPOSURE OF SEQUENTIAL PHOTOGRAPHS

Greenwich mean time, hr:min:sec	Report sequence	Film frame	Elapsed time from launch, sec
22:22:14.15900	1A	45	1634.45600
.19233	1B	46	.48933
.22566	1C	47	.52266
.25899	1D	48	.55599
.29232	1E	49	.58932
.32565	1F	50	.62265
22:22:15.15900	2A	75	1635.45600
.19233	2B	76	.48933
.22566	2C	77	.52266
.25899	2D	78	.55599
.29232	2E	79	.58932
.32565	2F	80	.62265
.35898	2G	81	.65598
.39231	2H	82	.68931
.42564	2I	83	.72264
.79167	3A	94	1636.08867
.82500	3B	95	.12200
.85833	3C	96	.15533
.89166	3D	97	.18866
.92499	3E	98	.22199
.95832	3F	99	.25532
22:22:16.79167	4A	124	1637.08867
.82500	4B	125	.12200
.85833	4C	126	.15533
.89166	4D	127	.18866
.92499	4E	128	.22199
.95832	4F	129	.25532
22:22:17.29100	5A	139	.58800
.32433	5B	140	.62133
.35766	5C	141	.65466
.39099	5D	142	.68799
.42432	5E	143	.72132
.45765	5F	144	.75465
.49098	5G	145	.78798
.52431	5H	146	.82131
.55764	5I	147	.85464
.59097	5J	148	.88797
.62430	5K	149	.92130
.65763	5L	150	.95463
.69096	5M	151	.98796
.72429	5N	152	1638.02129

APPENDIX A

TABLE A-II.- TIME OF EXPOSURE OF SEQUENTIAL PHOTOGRAPHS - Continued

Greenwich mean time, hr:min:sec	Report sequence	Film frame	Elapsed time from launch, sec
22:22:17.75762	5O	153	1638.05462
.79095	5P	154	.08795
.82428	5Q	155	.12128
.85761	5R	156	.15461
.89094	5S	157	.18794
.92427	5T	158	.22127
.95760	5U	159	.25460
.99093	5V	160	.28793
22:22:18.02426	5W	161	.32126
.05759	5X	162	.35459
.09092	5Y	163	.38792
.12425	5Z	164	.42125
.15758	5AA	165	.45458
.19091	5BB	166	.48791
.22424	5CC	167	.52124
.25757	5DD	168	.55457
.85833	6A	186	1639.15533
.89166	6B	187	.18866
.92499	6C	188	.22199
.95832	6D	189	.25532
.99165	6E	190	.28865
22:22:19.85833	7A	216	1640.15533
.89166	7B	217	.18866
.92499	7C	218	.22199
.95832	7D	219	.25532
.99165	7E	220	.28865
22:22:20.02498	7F	221	.32198
.05831	7G	222	.35531
.09164	7H	223	.38864
.12497	7I	224	.42197
22:22:22.15900	8A	285	1642.45600
.19233	8B	286	.48933
.22566	8C	287	.52266
.25899	8D	288	.55599
.29232	8E	289	.58932

## APPENDIX A

TABLE A-II.- TIME OF EXPOSURE OF SEQUENTIAL PHOTOGRAPHS - Continued

Greenwich mean time, hr:min:sec	Report sequence	Film frame	Elapsed time from launch, sec
22:22:22.32565	8F	290	1642.62265
.35898	8G	291	.65598
.39231	8H	292	.68931
.42564	8I	293	.72264
.45897	8J	294	.75597
.49230	8K	295	.78930
.52563	8L	296	.82263
22:22:23.15900	9A	315	1643.45600
.19233	9B	316	.48933
.22566	9C	317	.52266
22:22:24.25900	10A	348	1644.55590
.29233	10B	349	.58923
.32566	10C	350	.62256
22:22:25.15900	11A	375	1645.45600
.19233	11B	376	.48933
.22566	11C	377	.52266
.25899	11D	378	.55599
.29232	11E	379	.58932
.32565	11F	380	.62265
.52467	12A	386	.82167
.55800	12B	387	.85500
.59133	12C	388	.88833
.62466	12D	389	.92166
.65799	12E	390	.95499
.69132	12F	391	.98832
.72465	12G	392	1646.02165
.75798	12H	393	.05498
.79131	12I	394	.08831
22:22:26.55800	13A	417	.85500
.59133	13B	418	.88833
.62466	13C	419	.92166
.65799	13D	420	.95499
.69132	13E	421	.98832
.72465	13F	422	1647.02165

APPENDIX A

TABLE A-II.- TIME OF EXPOSURE OF SEQUENTIAL PHOTOGRAPHS - Concluded

Greenwich mean time, hr:min:sec	Report sequence	Film frame	Elapsed time, from launch, sec
22:22:27.15900	14A	435	1647.45600
.19233	14B	436	.48933
.22566	14C	437	.52266
.25899	14D	438	.55599
.29232	14E	439	.58932
.32565	14F	440	.62265
.79227	15A	454	1648.08927
.82560	15B	455	.12260
.85893	15C	456	.15593
.89226	15D	457	.18926
.92556	15E	458	.22259
.95892	15F	459	.25592
.99225	15G	460	.28925
22:22:28.02558	15H	461	.32258
.05891	15I	462	.35591
.09224	15J	463	.38924
.12557	15K	464	.42257
.15890	15L	465	.45590
.59229	16A	478	.88929
.62562	16B	479	.92262
.65895	16C	480	.95595
.69228	16D	481	.98928
.72561	16E	482	1649.02261
.75894	16F	483	.05594
.79227	16G	484	.08927
.82560	16H	485	.12260
.85893	16I	486	.15593
.89226	16J	487	.18926
.92556	16K	488	.22259
.95892	16L	489	.25592

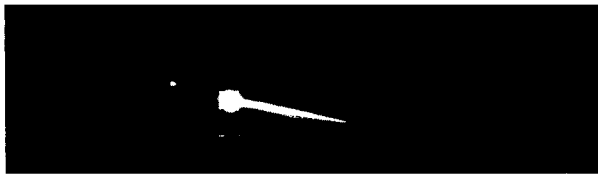
# APPENDIX A

## SEQUENCE 1: SIX PHOTOGRAPHS

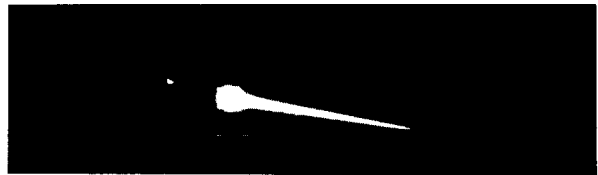
Sequence	Time after launch, sec
1A	1634.456
1B	1634.489
1C	1634.522
1D	1634.555
1E	1634.589
1F	1634.622

Sequence 1 shows the early gas light from both components of the spacecraft and the increasing separation distance between them. Flight direction is from right to left. The reentry package, shown as the small light flare on the left, is followed by the large flare and trailing wake of the spent velocity package consisting of the Antares case and the adapter section. The separation distance in sequence 1F is 236 meters.

During sequence 1 the reentry-package velocity changed from 11 350 m/sec at 1634.456 sec to 11 347 m/sec at 1634.622 sec.



1A



1D



1B



1E



1C



1F

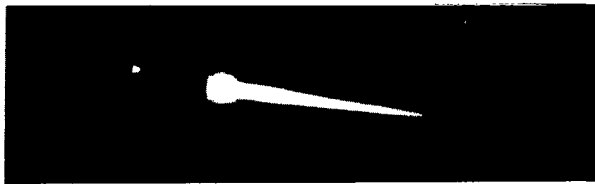
# APPENDIX A

## SEQUENCE 2: NINE PHOTOGRAPHS

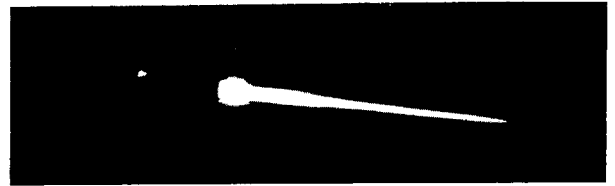
Sequence	Time after launch, sec
2A	1635.456
2B	1635.489
2C	1635.522
2D	1635.555
2E	1635.589
2F	1635.622
2G	1635.655
2H	1635.689
2I	1635.722

Sequence 2 displays the increasing gas light from the spent Antares and the velocity package components and indicates some early outgassing or afterbody surface ablation from the reentry package. Separation distance in photograph 2I is 328 meters.

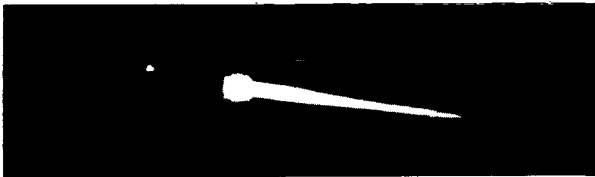
During sequence 2 the reentry-package velocity changed from 11 329 m/sec at 1635.456 sec to 11 322 m/sec at 1635.722 sec.



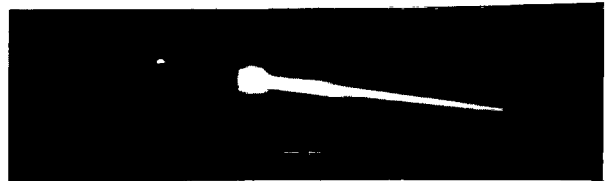
2A



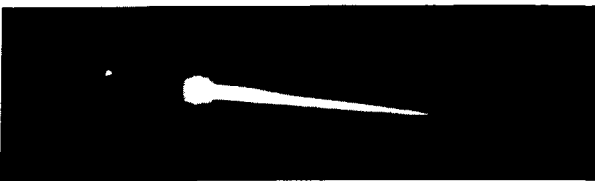
2D



2B



2E

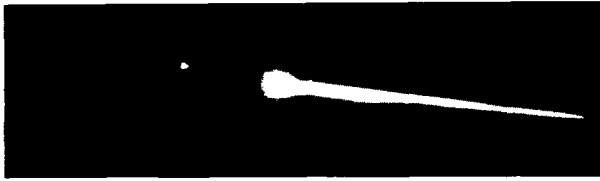


2C

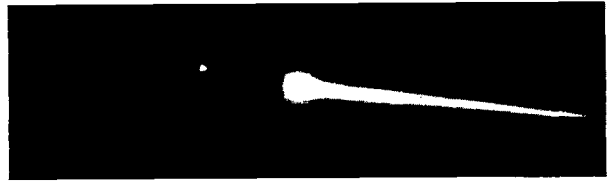


2F

APPENDIX A



2G



2H



2I

SEQUENCE 3: SIX PHOTOGRAPHS

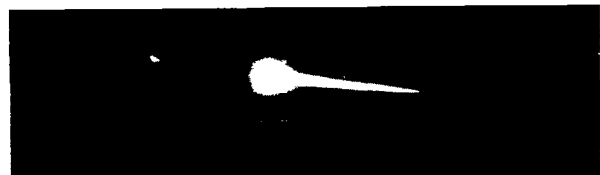
Sequence	Time after launch, sec
3A	1636.089
3B	1636.122
3C	1636.155
3D	1636.188
3E	1636.221
3F	1636.255

The photographs of sequence 3 demonstrate the effects of tumbling action on the spent Antares rocket case and the reentry-package adapter. The intense flare observed in photograph 3C followed by an increasing visible wake in photographs 3E and 3F show results of tumbling. The separation distance between the reentry package and spent Antares has increased to 400 meters in photograph 3F. The visible wake of photograph 3F is approximately 1400 meters in length.

During sequence 3 the reentry-package velocity changed from 11 311 m/sec at 1636.089 sec to 11 305 m/sec at 1636.255 sec.

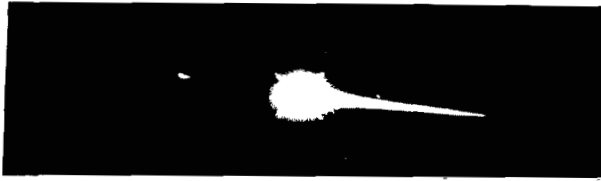


3A



3B

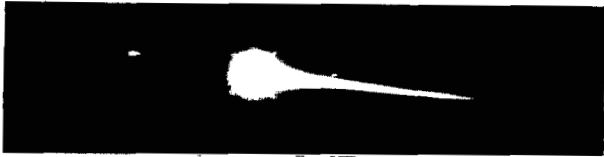
APPENDIX A



3 C



3 E



3 D



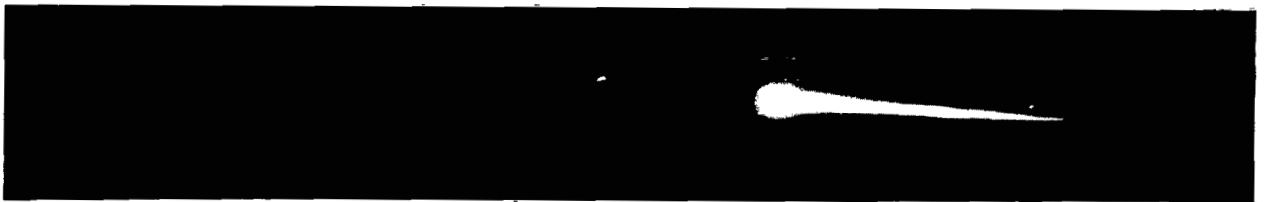
3 F

SEQUENCE 4: SIX PHOTOGRAPHS

Sequence	Time after launch, sec
4A	1637.089
4B	1637.122
4C	1637.155
4D	1637.188
4E	1637.221
4F	1637.255

Sequence 4 continues to demonstrate the severe effects of tumbling by the flareup of the spent Antares (photograph 4C) and the beginning of breakup noted by separate pieces appearing to burn in the wake. Because of apparent camera motion this sequence was not used for separation measurements, but even with the camera motion the separation distance can be determined to be in excess of 450 meters and the spent Antares wake length in excess of 1400 meters.

During sequence 4 the reentry-package velocity changed from 11 271 m/sec at 1637.089 sec to 11 263 m/sec at 1637.255 sec.

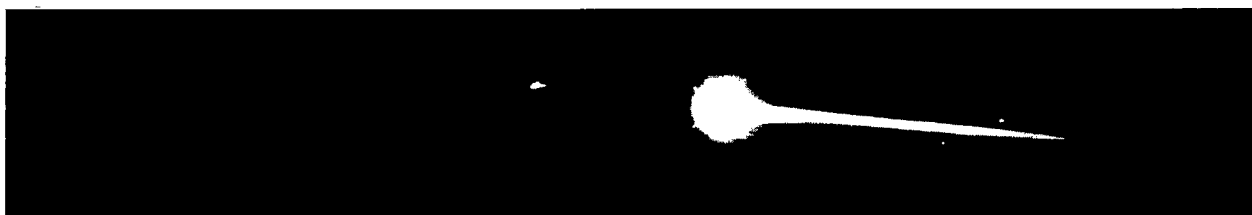


4 A

APPENDIX A



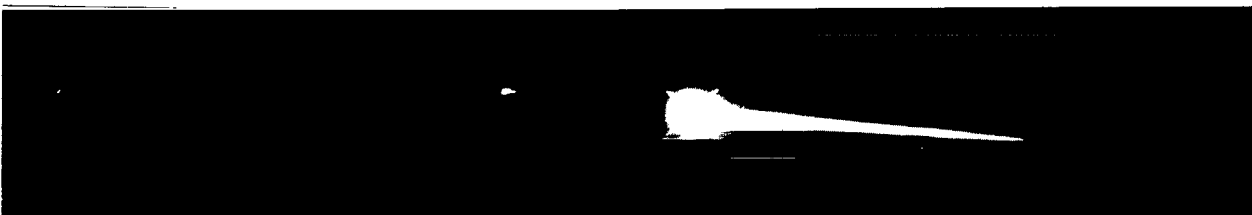
4B



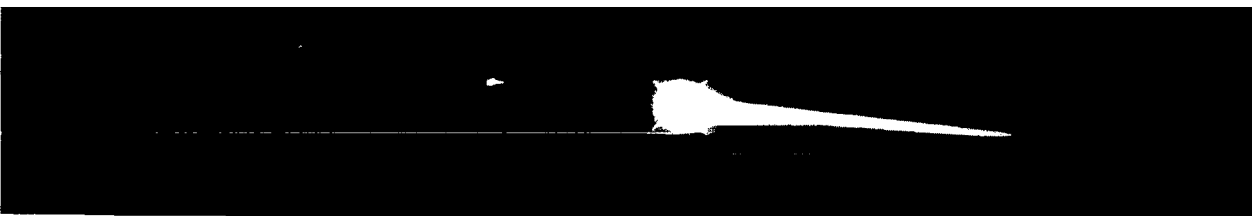
4C



4D



4E



4F

## APPENDIX A

### SEQUENCE 5: 30 PHOTOGRAPHS

Sequence 5 consists of 30 photographs recorded from 1637.588 seconds elapsed time from lift-off until 1638.554 seconds. The time interval between sequential photographs is 0.0333 second. During this time interval the separation distance between the reentry package and spent Antares increased from 625 meters to 815 meters. The visible wake from the disintegrating and burning spent Antares components fluctuates between 1500 and 2000 meters.

During sequence 5 the reentry-package velocity changed from 11 245 m/sec at 1637.588 sec to 11 182 m/sec at 1638.554 sec.



5 A



5 B

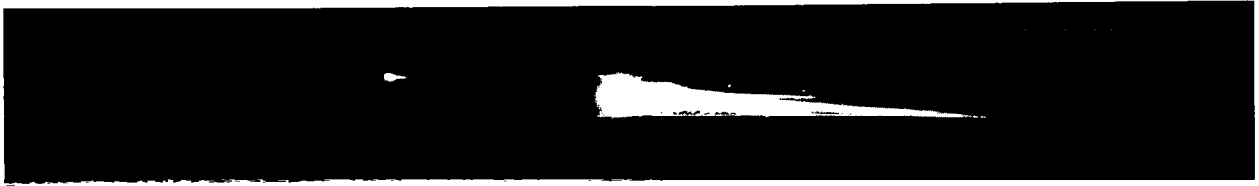


5 C

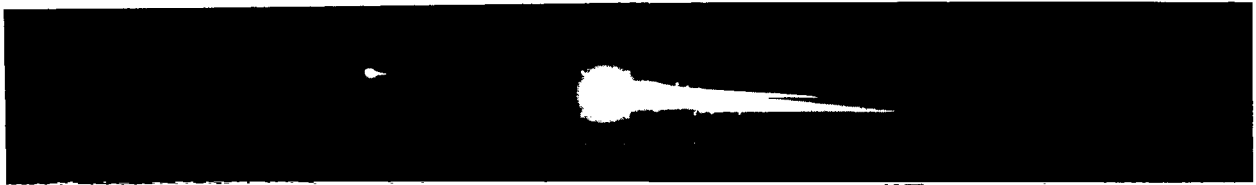


5 D

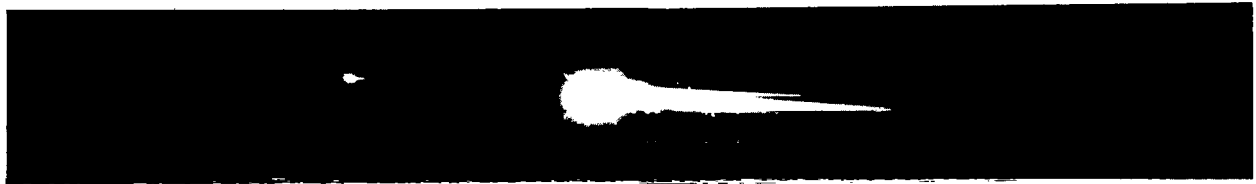
APPENDIX A



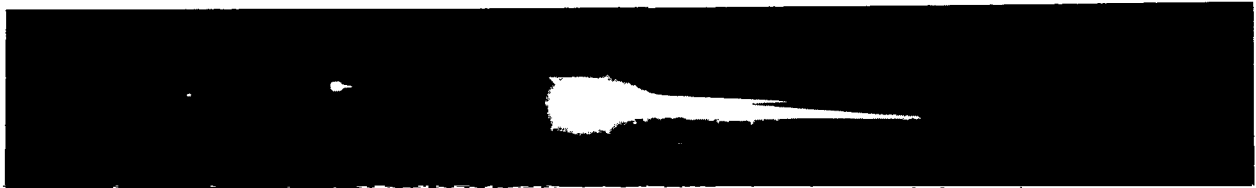
5 E



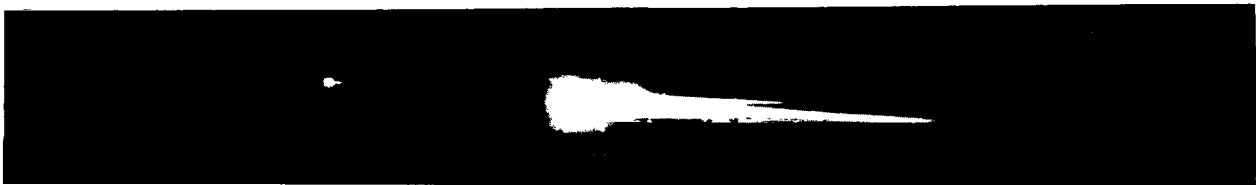
5 F



5 G



5 H



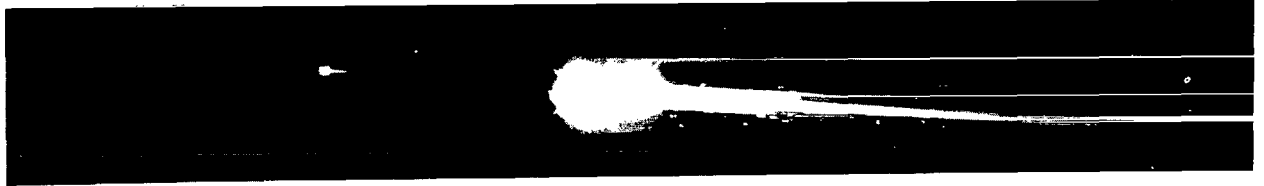
5 I

Beginning with photograph 5J at 1637.887 seconds, an object can be noticed breaking away from the main body of the spent Antares section. Because of its higher  $W/C_{DA}$ , it is not being decelerated as rapidly as the larger portions.

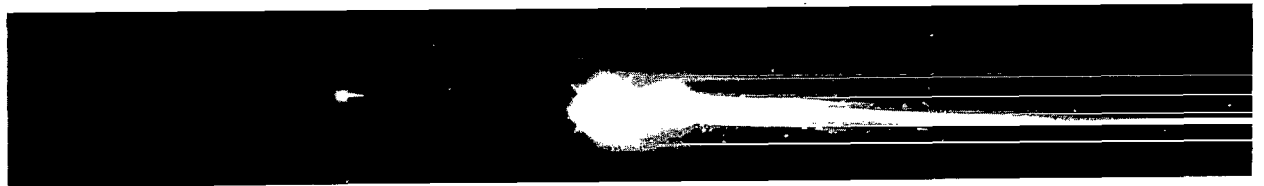
APPENDIX A



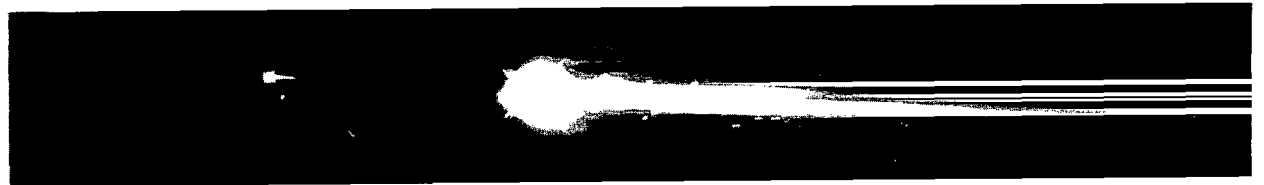
5 J



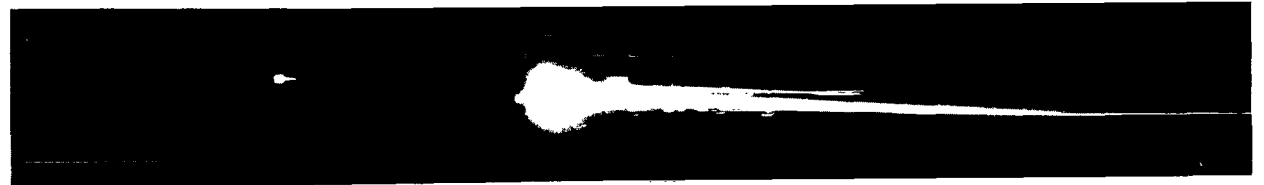
5 K



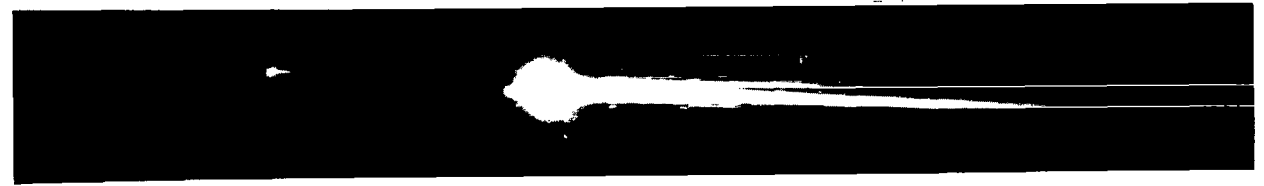
5 L



5 M



5 N



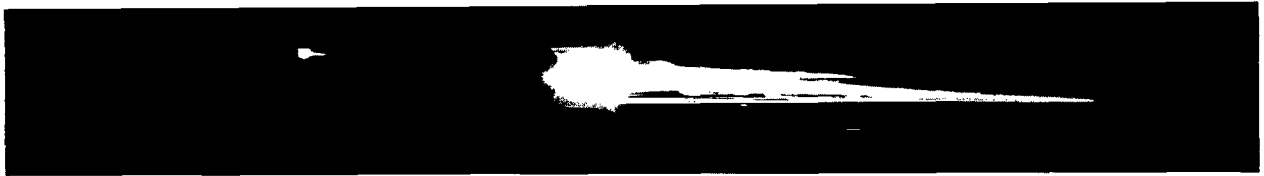
5 O

APPENDIX A

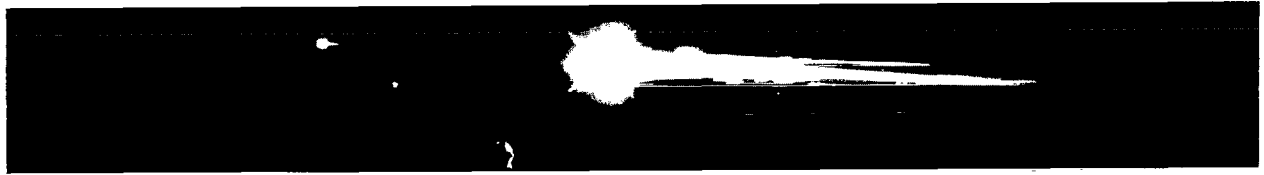


5P

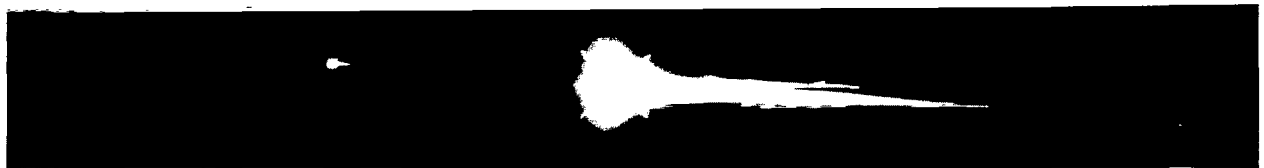
In photograph 5Q at 1638.121 seconds, a second object begins to move in front of the large mass of glowing Antares components. This second object appears smaller than the first and is identified from color photography as the brass drag plate counterbalance. It can be observed that this object by its greater  $W/C_{DA}$  rapidly moves in front of the other objects and is visible for a longer period than the larger object which first appeared on photograph 5J. The rapidly changing intensity pattern of the spent Antares caused by the tumbling attests to the effectiveness of the tumble motor and drag plate for increasing the separation between the reentry package and the spent Antares.



5Q

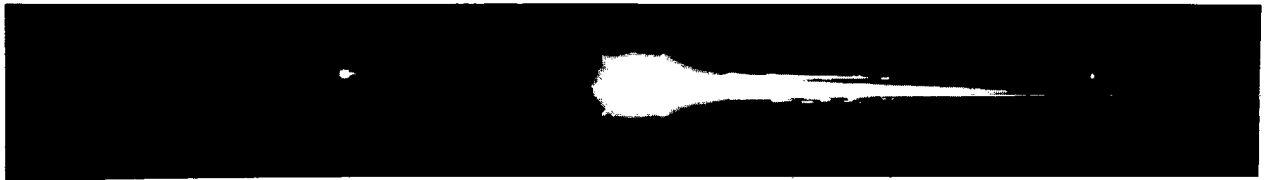


5R

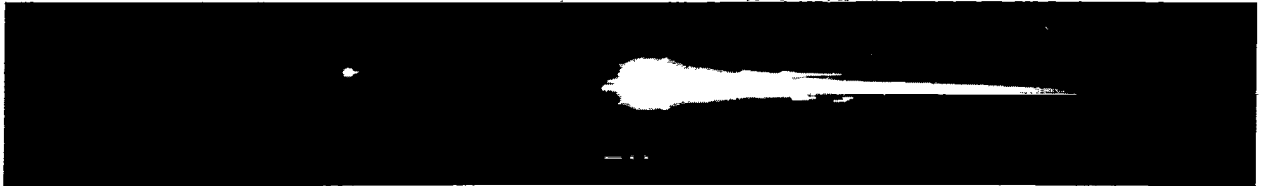


5S

APPENDIX A



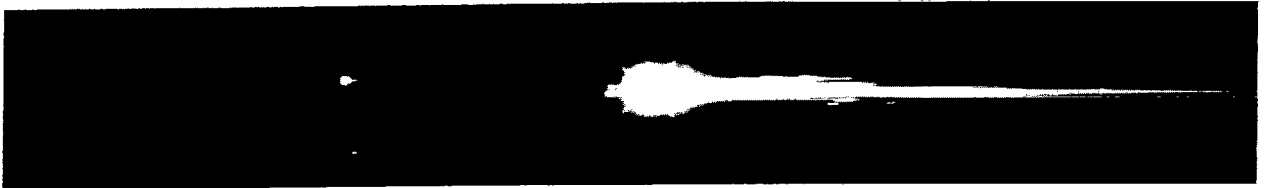
5T



5U



5V



5W



5X

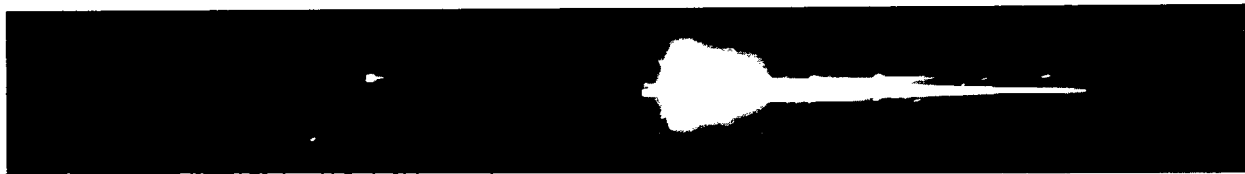


5Y

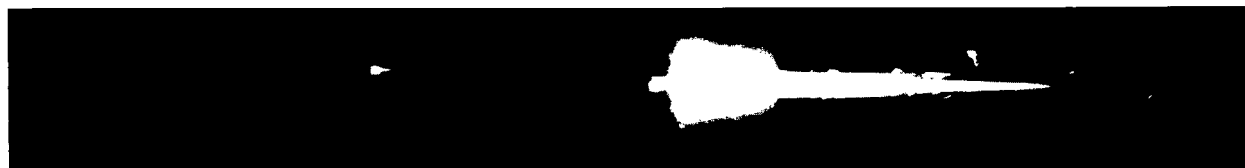
APPENDIX A



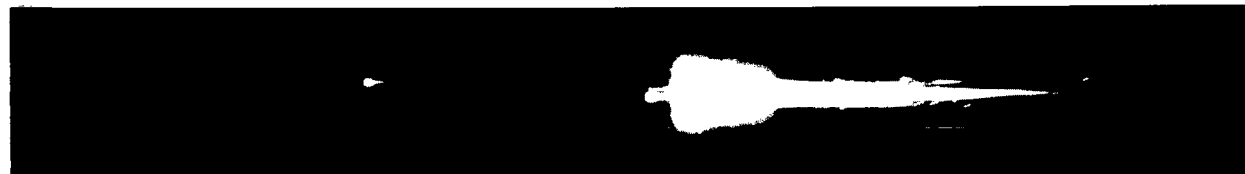
5Z



5AA

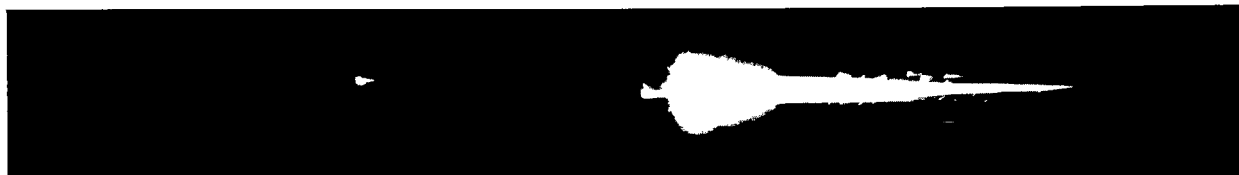


5BB



5CC

The disintegration of the spent Antares continues with an indication of increased effects of atmospheric heating. At 1638.554 (photograph 5DD) or 20.8 seconds after passing through 121 920 meters, the reentry package is experiencing a 7.9g deceleration while the larger portion of the spent Antares is experiencing a 8.3g deceleration.



5DD

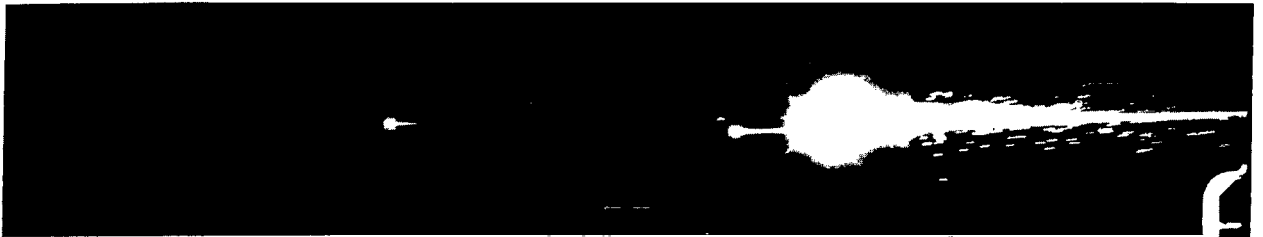
## APPENDIX A

### SEQUENCE 6: FIVE PHOTOGRAPHS

Sequence	Time after launch, sec
6A	1639.155
6B	1639.188
6C	1639.221
6D	1639.255
6E	1639.288

The photographs of sequence 6 began 0.04 second after activation of the reentry timer. The timer was activated when the reentry package experienced a 10.4g deceleration. During this sequence, severe breakup of the spent Antares is apparent. The separation distance between components continues to increase, and outgassing and afterbody ablation of the reentry package becomes more pronounced. The separation distance between the reentry package and the nearest separated piece of the spent Antares has increased to a distance of 925 meters in photograph 6E.

During sequence 6, the reentry-package velocity changed from 11 130 m/sec at 1639.155 sec to 11 117 m/sec at 1639.288 sec.



6 A



6 B

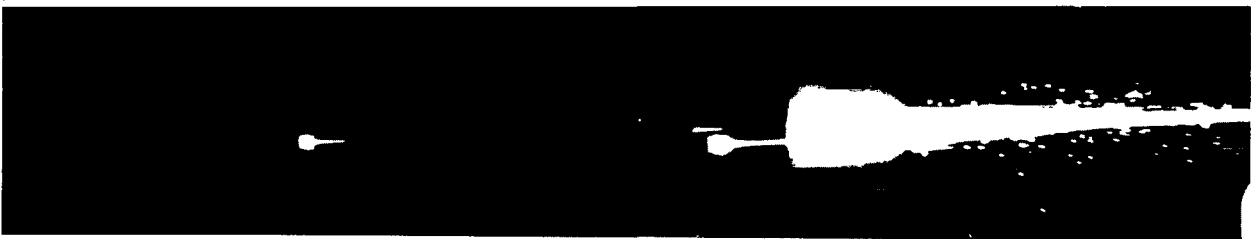
APPENDIX A



6 C



6 D



6 E

SEQUENCE 7: NINE PHOTOGRAPHS

Sequence	Time after launch, sec
7A	1640.155
7B	1640.188
7C	1640.221
7D	1640.255
7E	1640.288
7F	1640.321
7G	1640.355
7H	1640.388
7I	1640.421

## APPENDIX A

Sequence 7 does not show the reentry package, since it has moved out of the field of view to the left. This sequence provides the first indication of the melting beryllium calorimeter as a bright well-defined wake. On the color photographs, this wake is distinguished by its red color. Prelaunch calculations predicted that the beryllium should begin to melt at 1640 seconds, and the photograph recorded first visible indication of melting beryllium at 1640.155 seconds.

During sequence 7 the reentry-package velocity changed from 11 020 m/sec at 1640.155 sec to 10 984 m/sec at 1640.421 sec.



7A



7B



7C

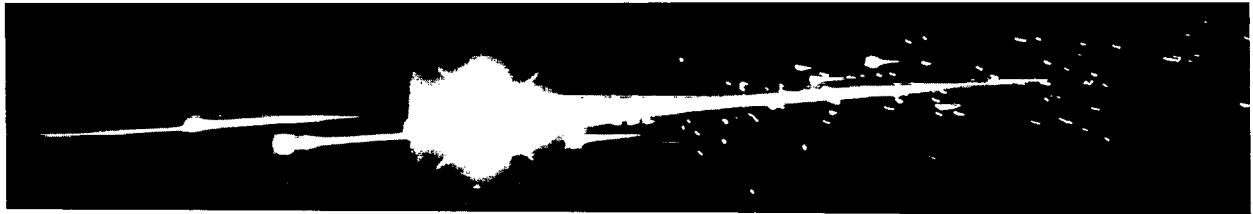


7D

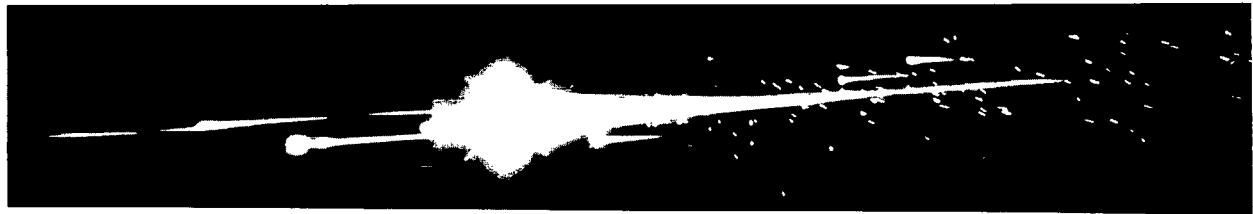
APPENDIX A



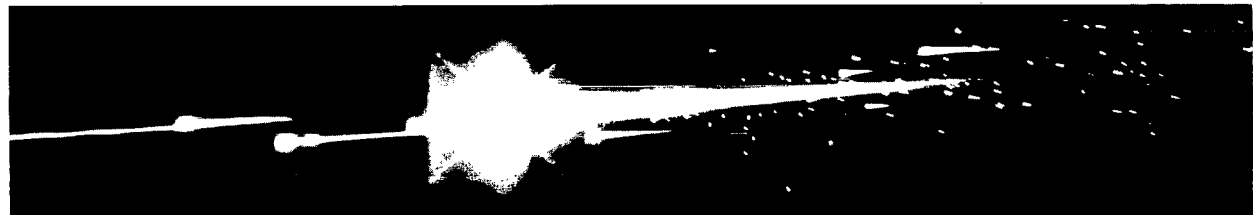
7 E



7 F



7 G



7 H



7 I

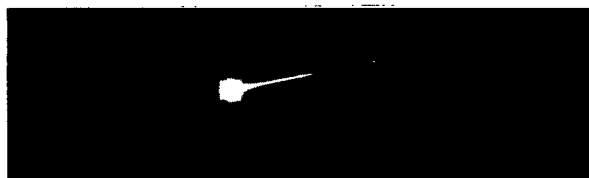
## APPENDIX A

### SEQUENCE 8: 12 PHOTOGRAPHS

Sequence	Time after launch, sec
8A	1642.456
8B	1642.489
8C	1642.522
8D	1642.555
8E	1642.589
8F	1642.622
8G	1642.655
8H	1642.689
8I	1642.722
8J	1642.755
8K	1642.788
8L	1642.822

Sequence 8 shows only the reentry package, as the separation distance between the reentry package and the spent Antares has increased to a distance greater than can be covered by the camera field of view. This sequence shows the final melt-off of the first beryllium calorimeter and the ejection of the first phenolic asbestos ablation shield. The later photographs of this series show the clean nonablating reentry package after the ablation shield has separated.

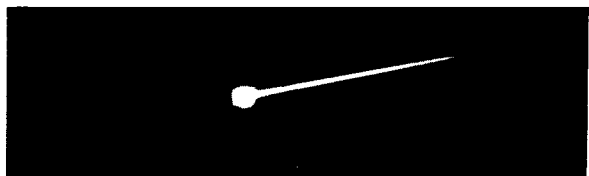
During sequence 8, the reentry-package velocity changed from 10 613 m/sec at 1642.456 to 10 523 m/sec at 1642.822 sec.



8A



8C

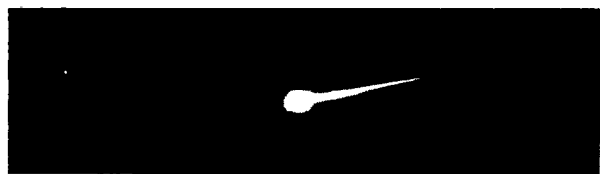


8B



8D

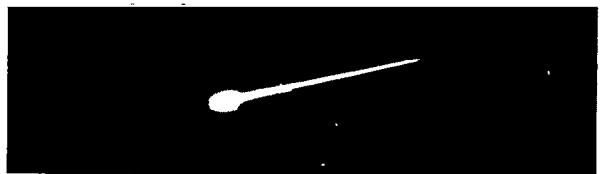
## APPENDIX A



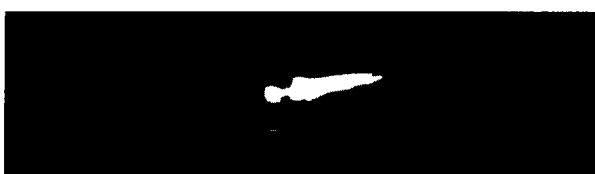
8E



8I



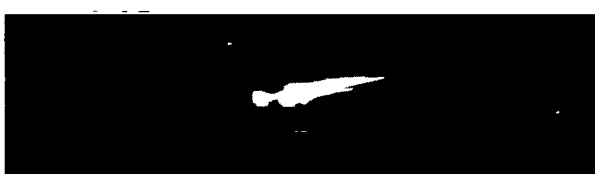
8F



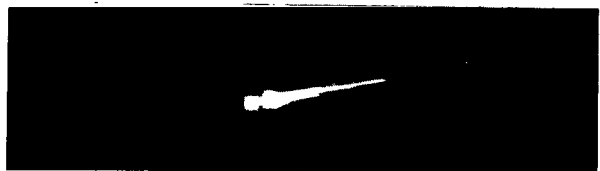
8J



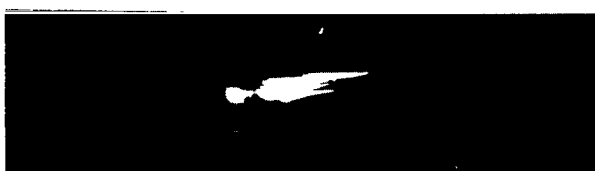
8G



8K



8H



8L

### SEQUENCE 9: THREE PHOTOGRAPHS

Sequence	Time after launch, sec
9A	1643.456
9B	1643.489
9C	1643.522

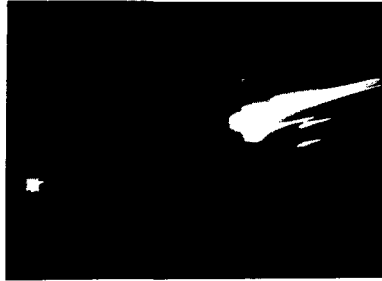
The photographs of sequence 9 show the reentry package during the early portion of the second data period and the burning phenolic ablation shield which was ejected to expose a clean second calorimeter.

During sequence 9 the reentry-package velocity changed from 10 354 m/sec at 1643.456 sec to 10 334 m/sec at 1643.522 sec.

## APPENDIX A



9A



9B



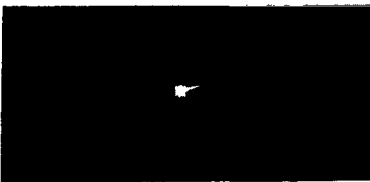
9C

### SEQUENCE 10: THREE PHOTOGRAPHS

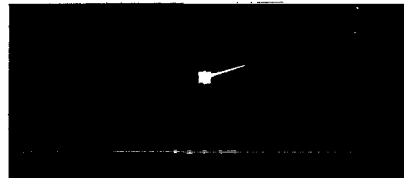
Sequence	Time after launch, sec
10A	1644.555
10B	1644.589
10C	1644.622

The photographs of sequence 10 show the beginning of ablation during the second data period prior to melting of the second calorimeter.

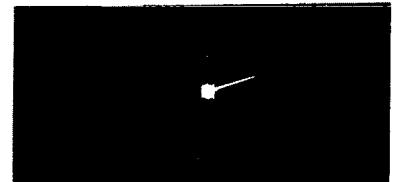
During sequence 10 the reentry-package velocity changed from 9 998 m/sec at 1644.555 to 9 972 m/sec at 1644.622 sec.



10A



10B



10C

### SEQUENCE 11: SIX PHOTOGRAPHS

Sequence	Time after launch, sec
11A	1645.456
11B	1645.489
11C	1645.522
11D	1645.555
11E	1645.589
11F	1645.622

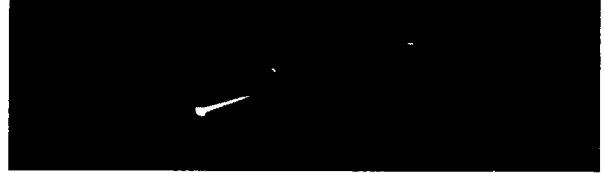
## APPENDIX A

Sequence 11 shows the beginning of melting of the second beryllium calorimeter. Prelaunch calculations predicted that melting of the second beryllium calorimeter should begin at 1645.5 seconds.

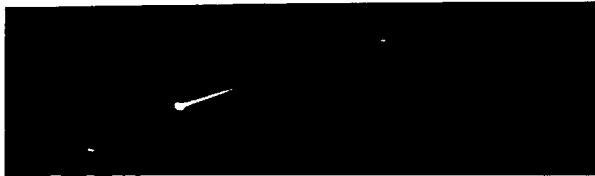
During sequence 11 the reentry-package velocity changed from 9 648 m/sec at 1645.456 sec to 9 573 m/sec at 1645.622 sec.



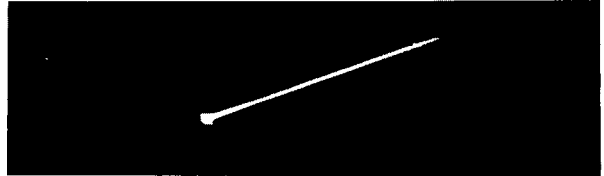
IIA



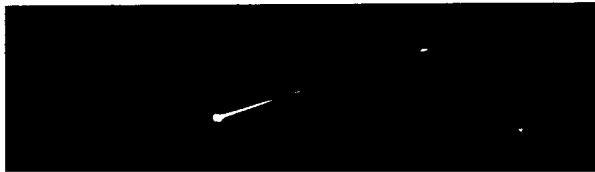
IID



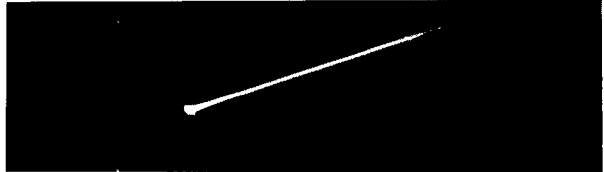
IIB



IIE



IIC



IIF

### SEQUENCE 12: NINE PHOTOGRAPHS

Sequence	Time after launch, sec
12A	1645.822
12B	1645.855
12C	1645.888
12D	1645.921
12E	1645.954
12F	1645.988
12G	1646.021
12H	1646.054
12I	1646.088

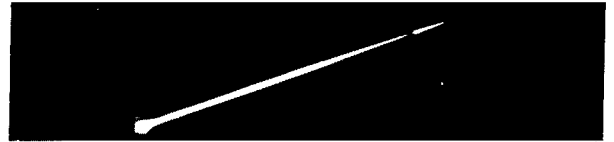
## APPENDIX A

Sequence 12 shows the melt of the second beryllium calorimeter. The visible wake of the melting beryllium in this series is approximately 760 meters in length.

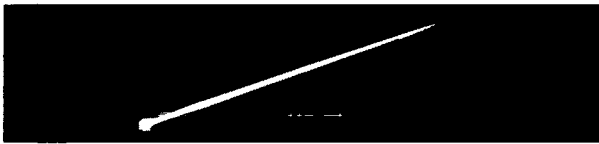
During sequence 12 the reentry-package velocity changed from 9 485 m/sec at 1645.822 sec to 9 367 m/sec at 1646.088 sec.



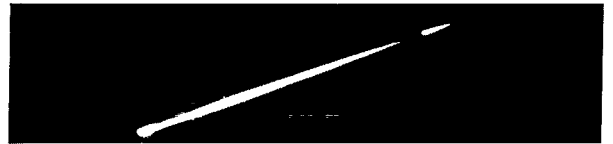
12 A



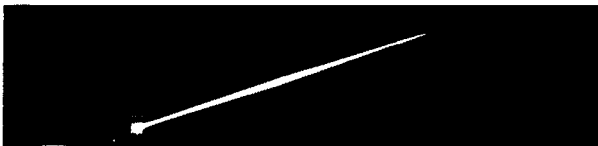
12 E



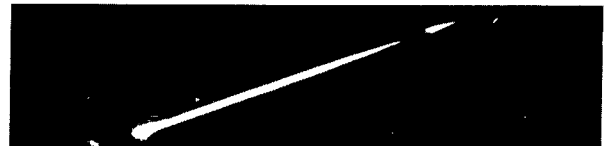
12 B



12 F



12 C



12 G



12 D



12 H



12 I

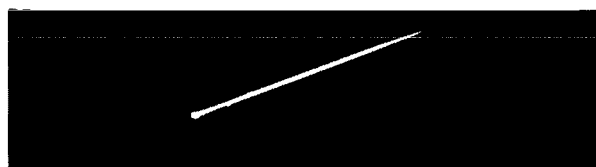
APPENDIX A

SEQUENCE 13: SIX PHOTOGRAPHS

Sequence	Time after launch, sec
13A	1646.855
13B	1646.888
13C	1646.921
13D	1646.954
13E	1646.988
13F	1647.021

Sequence 13 shows the continuing melt of the second beryllium calorimeter layer and photographs 13B and 13C show indication of a segment of beryllium coming off from the reentry package.

During sequence 13 the reentry-package velocity changed from 8 975 m/sec at 1646.855 to 8 884 m/sec at 1647.021 sec.



13A



13D



13B



13E



13C



13F

## APPENDIX A

### SEQUENCE 14: SIX PHOTOGRAPHS

Sequence	Time after launch, sec
14A	1647.456
14B	1647.489
14C	1647.522
14D	1647.555
14E	1647.589
14F	1647.622

Sequence 14 shows continuing melt of the second beryllium calorimeter with a segment of beryllium flaring up and burning off in photographs 14C and 14D. It is probable that the segment was caused to separate by the ignition of the pyrofuze link which ejects the second ablation shield. The pyrofuze signal was initiated at 1647.5 seconds and photograph 14C was recorded at 1647.522 seconds.

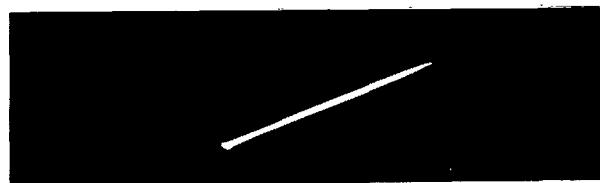
During sequence 14 the reentry-package velocity changed from 8 638 m/sec at 1647.456 sec to 8 535 m/sec at 1647.622 sec.



14A



14D



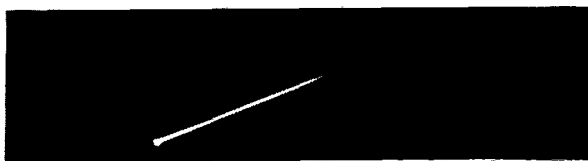
14B



14E



14C



14F

## APPENDIX A

### SEQUENCE 15: 12 PHOTOGRAPHS

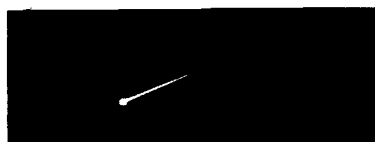
Sequence	Time after launch, sec
15A	1648.089
15B	1648.122
15C	1648.155
15D	1648.189
15E	1648.222
15F	1648.255
15G	1648.288
15H	1648.321
15I	1648.354
15J	1648.387
15K	1648.421
15L	1648.454

Sequence 15 shows the melt of the remaining beryllium of the second calorimeter, the first visible indication of second ablation-shield ejection, and the ejection and burn of the second phenolic ablation shield. Photographs 15C and 15D show a segment of melting beryllium, which was most likely disturbed by the beginning of ablation-shield ejection. Photograph 15E shows the first indication of the ablation-shield segments passing behind the reentry package. This separation between reentry package and shield segments is well defined in photographs 15F, 15G, and 15H. Photographs 15I, 15J, 15K, and 15L show the many pieces of ablation shield which have been ejected as they first begin to burn intensely and then appear to cool rapidly rather than being completely consumed.

During sequence 15 the reentry-package velocity changed from 8 251 m/sec at 1648.089 sec to 8 007 m/sec at 1648.454 sec.



15 A



15 B



15 C



15 D



15 E

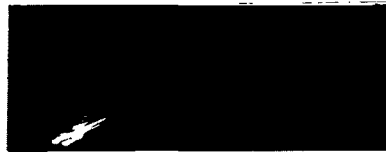


15 F

APPENDIX A



15 G



15 H



15 I



15 J



15 K



15 L

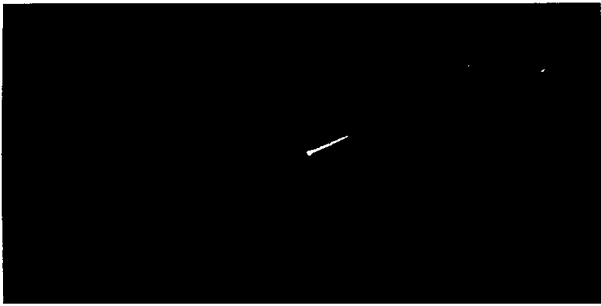
SEQUENCE 16: 12 PHOTOGRAPHS

Sequence	Time after launch, sec
16A	1648.889
16B	1648.922
16C	1648.955
16D	1648.989
16E	1649.022
16F	1649.055
16G	1649.089
16H	1649.122
16I	1649.155
16J	1649.189
16K	1649.222
16L	1649.255

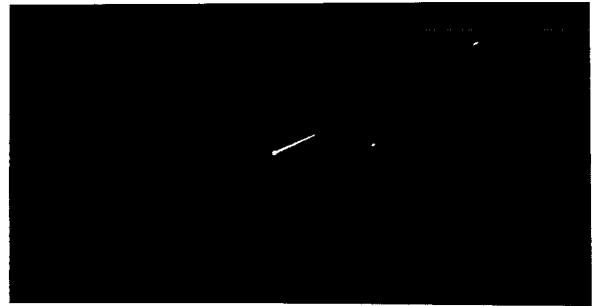
Sequence 16 shows the reentry package during the early portion of the third data period. Portions of the ejected phenolic asbestos ablation shield may be seen following the reentry package. A comparison between photographs 9B and 16A demonstrates the different intensities of heating during the second and third data periods. Photograph 9B was recorded 1.369 seconds following the first ablation-shield eject signal and photograph 16A was recorded 1.359 seconds following the second ablation-shield eject signal.

During sequence 16 the reentry-package velocity changed from 7 713 m/sec at 1648.889 sec to 7 451 m/sec at 1649.255 sec.

APPENDIX A



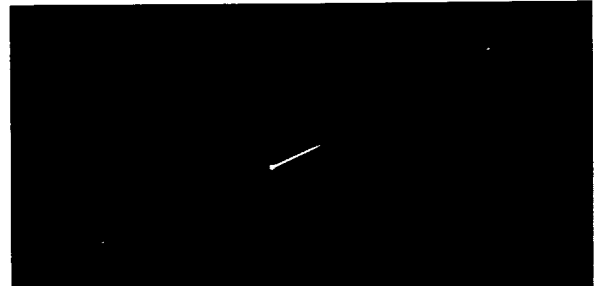
16 A



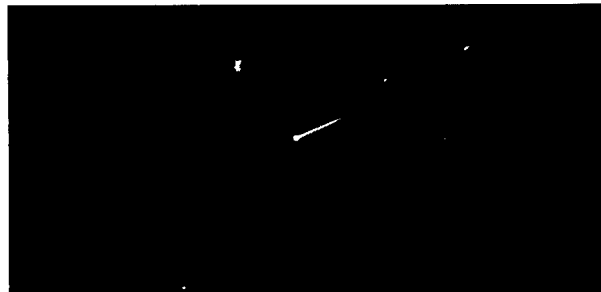
16 E



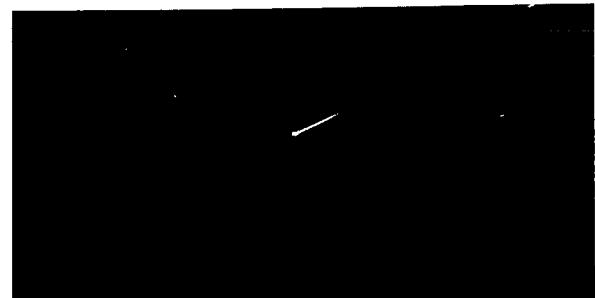
16 B



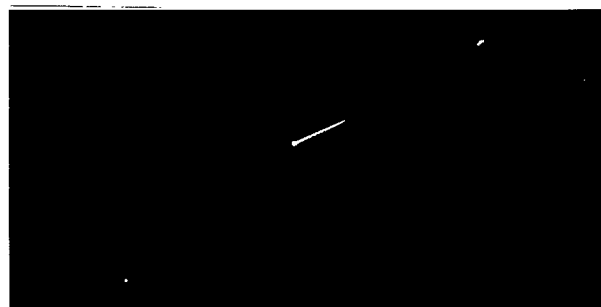
16 F



16 C



16 G



16 D

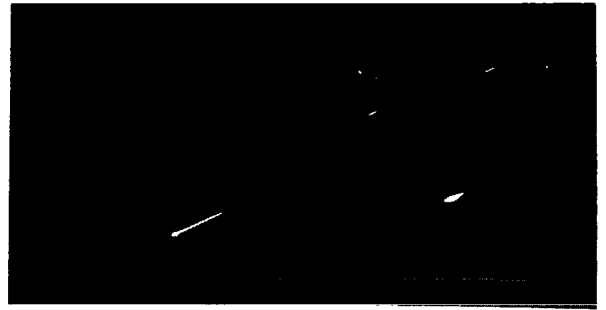


16 H

APPENDIX A



16 I



16 K



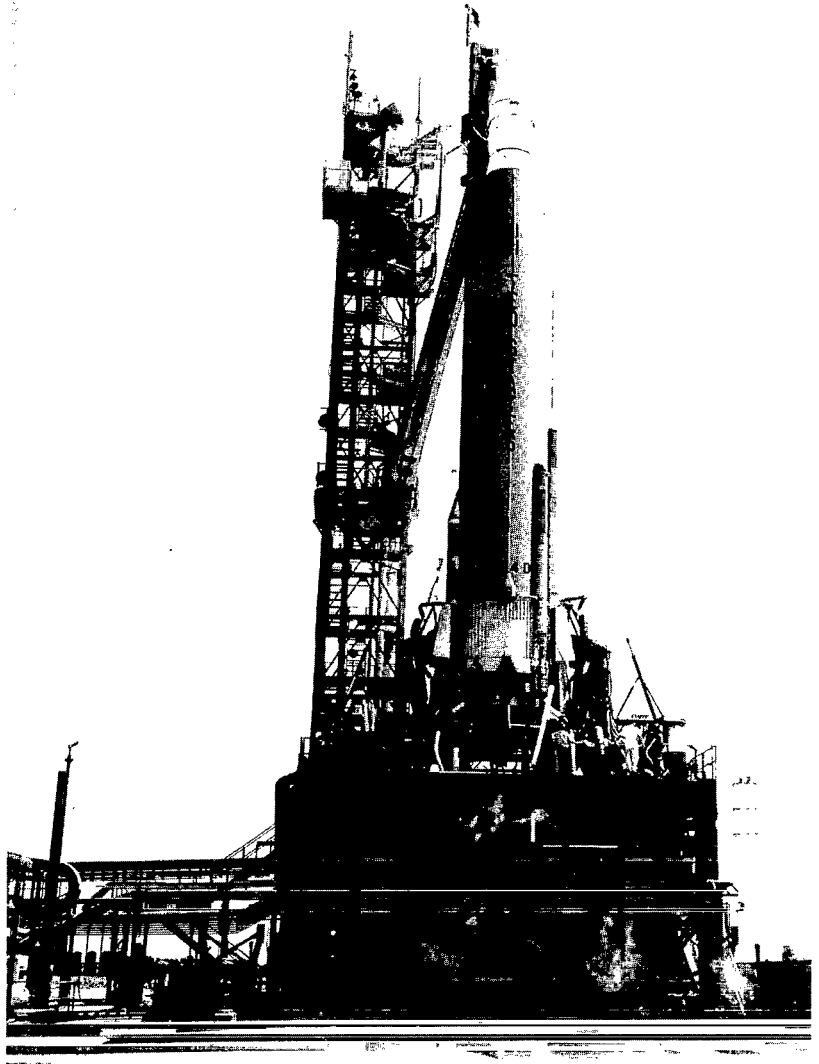
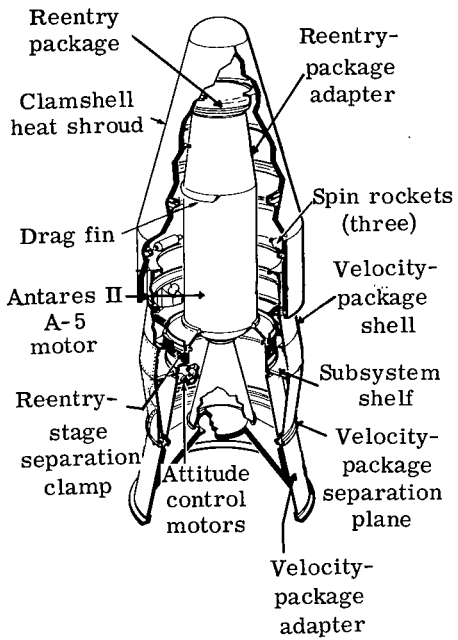
16 J



16 L

## REFERENCES

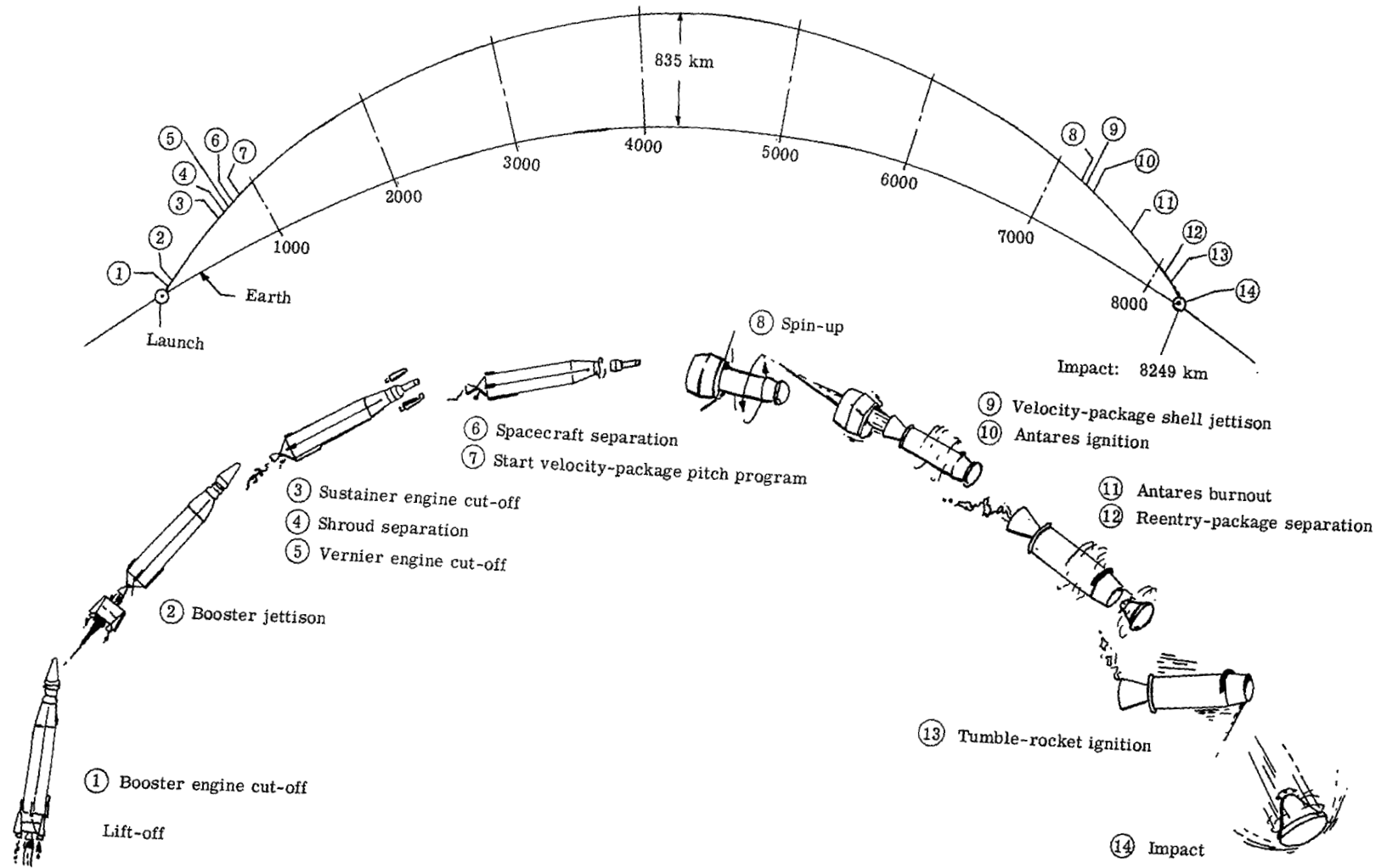
1. Scallion, William I.; and Lewis, John H., Jr.: Flight Parameters and Vehicle Performance for Project Fire Flight 1, Launched April 14, 1964. NASA TN D-2996, 1965.
2. Cornette, Elden S.: Forebody Temperatures and Total Heating Rates Measured During Project Fire 1 Reentry at 38 000 Feet Per Second. NASA TM X-1120, 1965.
3. Signature Processing: Optical Signature Data Report 65-020 for Test 0501 (Project Fire). Vols. I-III, RCA Serv. Co., A.F. Eastern Test Range, Nov. 5, 1965.
4. Popper, L. A.; Mahoney, P. A.; Playdon, R. T.; Bankoff, M. L.; and Staal, J. V.: Re-Entry Data Report - Project Fire (14 April 1964). Res. Note 503, Avco-Everett Res. Lab., Jan. 1965.



(a) Launch configuration and cutaway view of spacecraft.

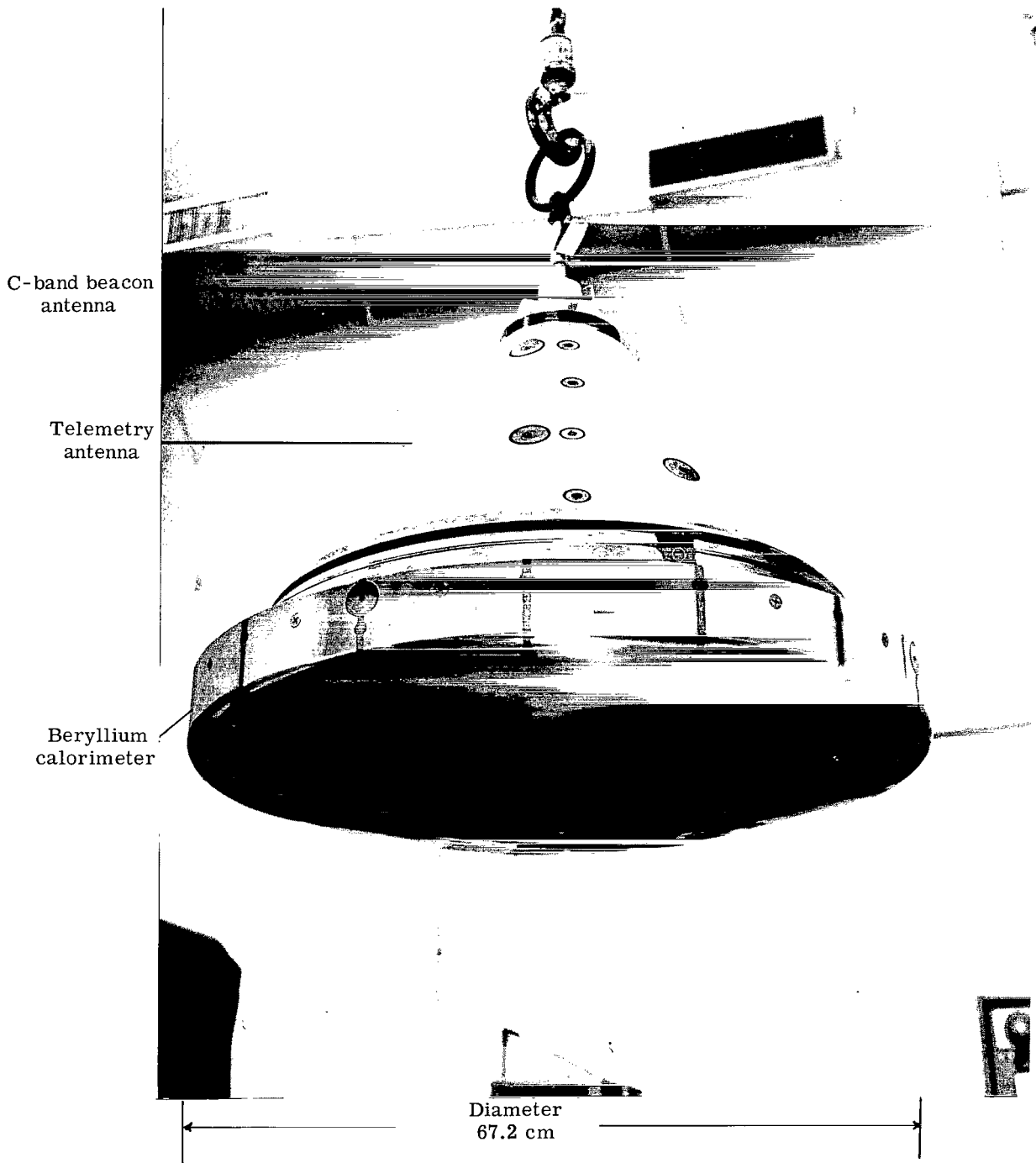
L-66-4441

Figure 1.- Project Fire space vehicle.



(b) Vehicle trajectory and flight sequence of events.

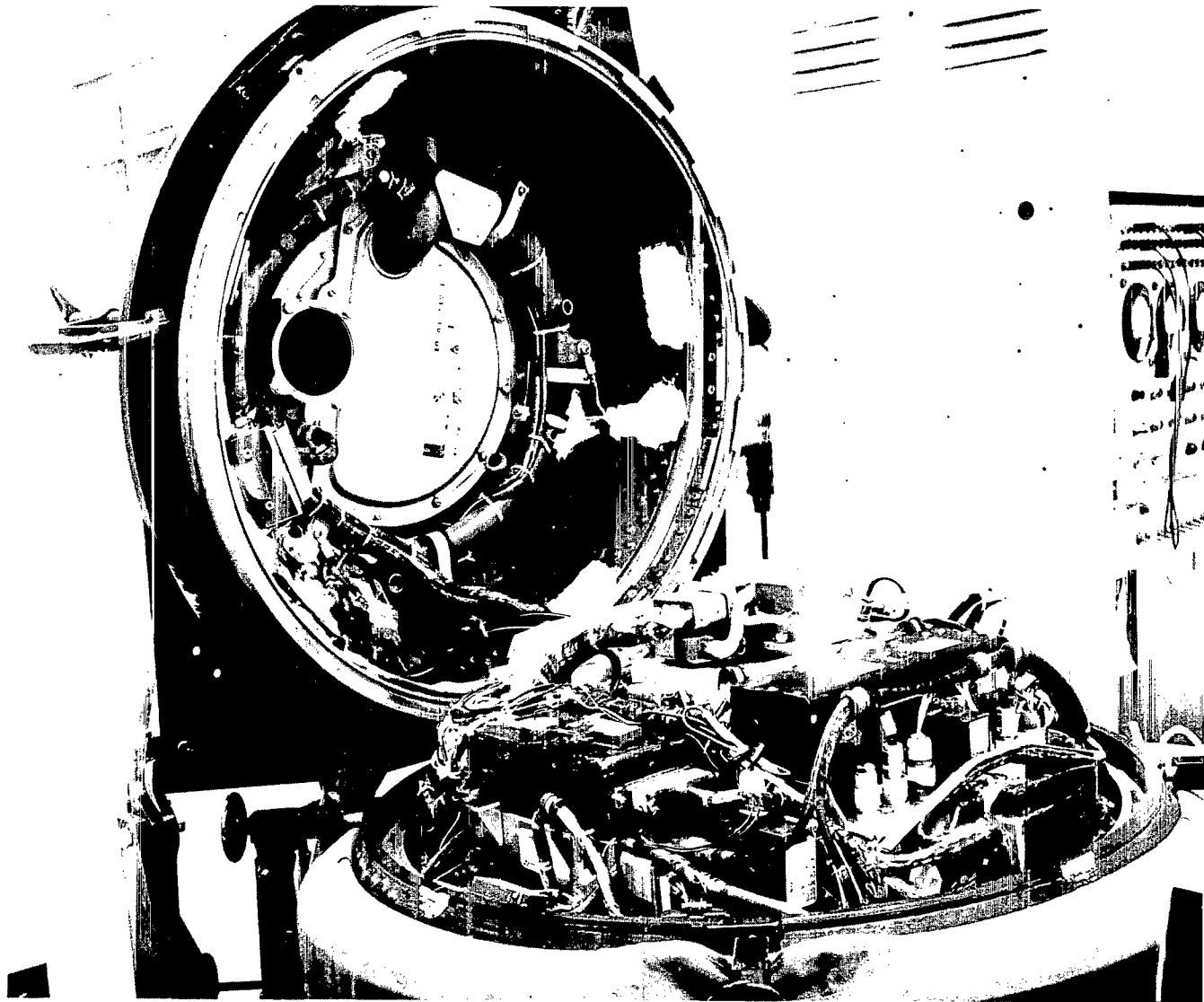
Figure 1.- Concluded.



(a) Exterior view.

L-66-4442

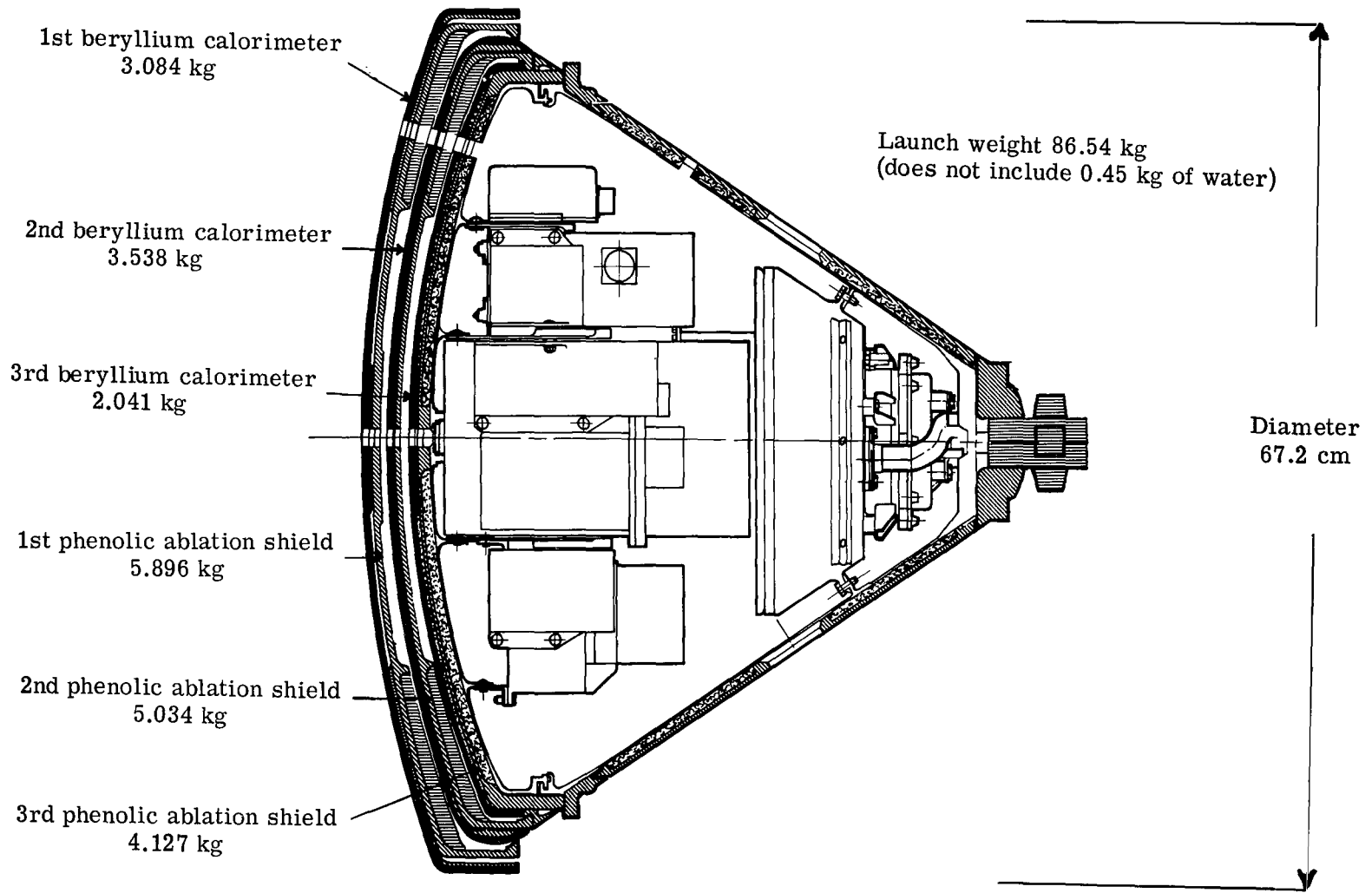
Figure 2.- Reentry package.



(b) Interior view.

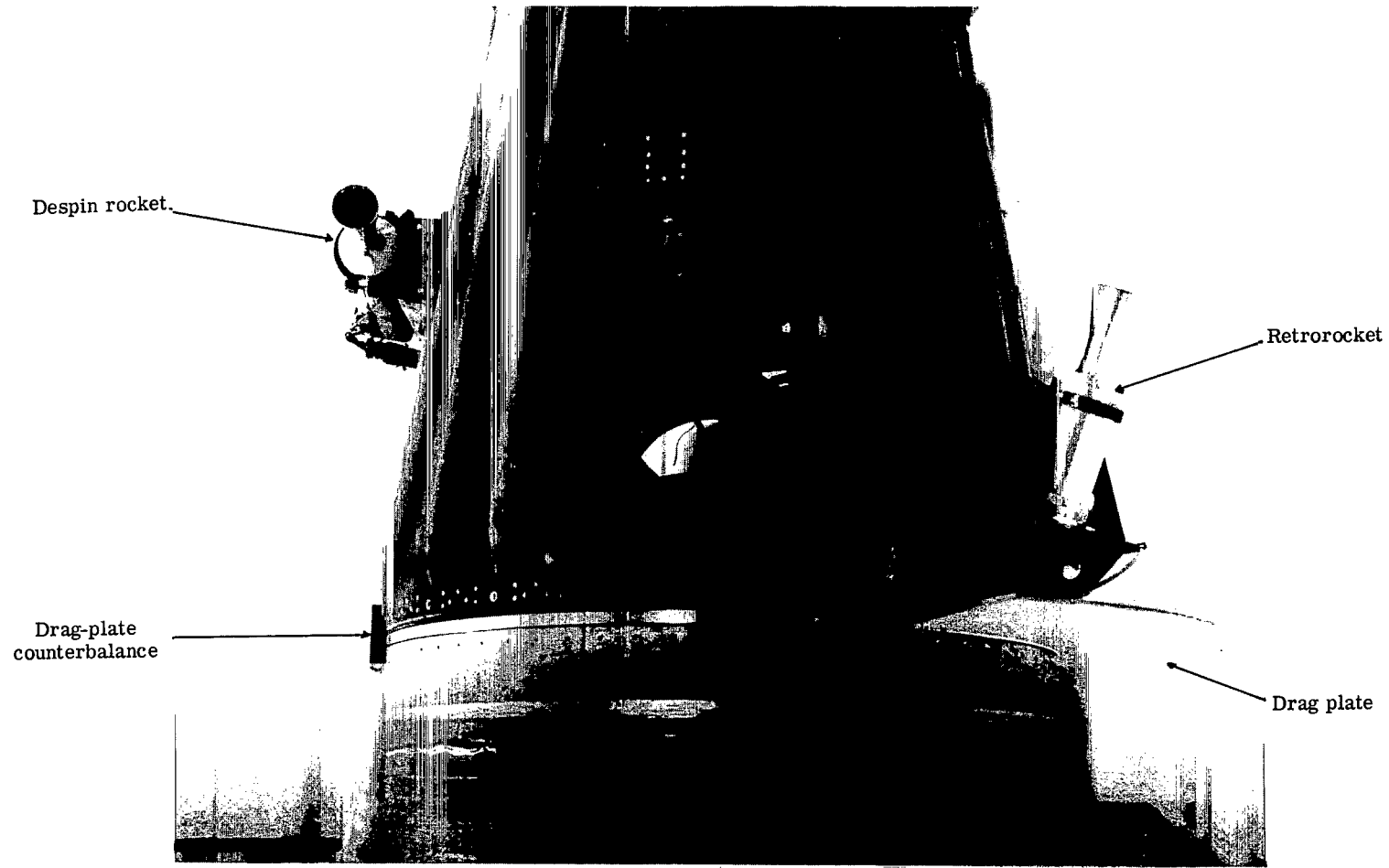
L-66-4443

Figure 2.- Continued.



(c) Sectional sketch showing reentry-package details.

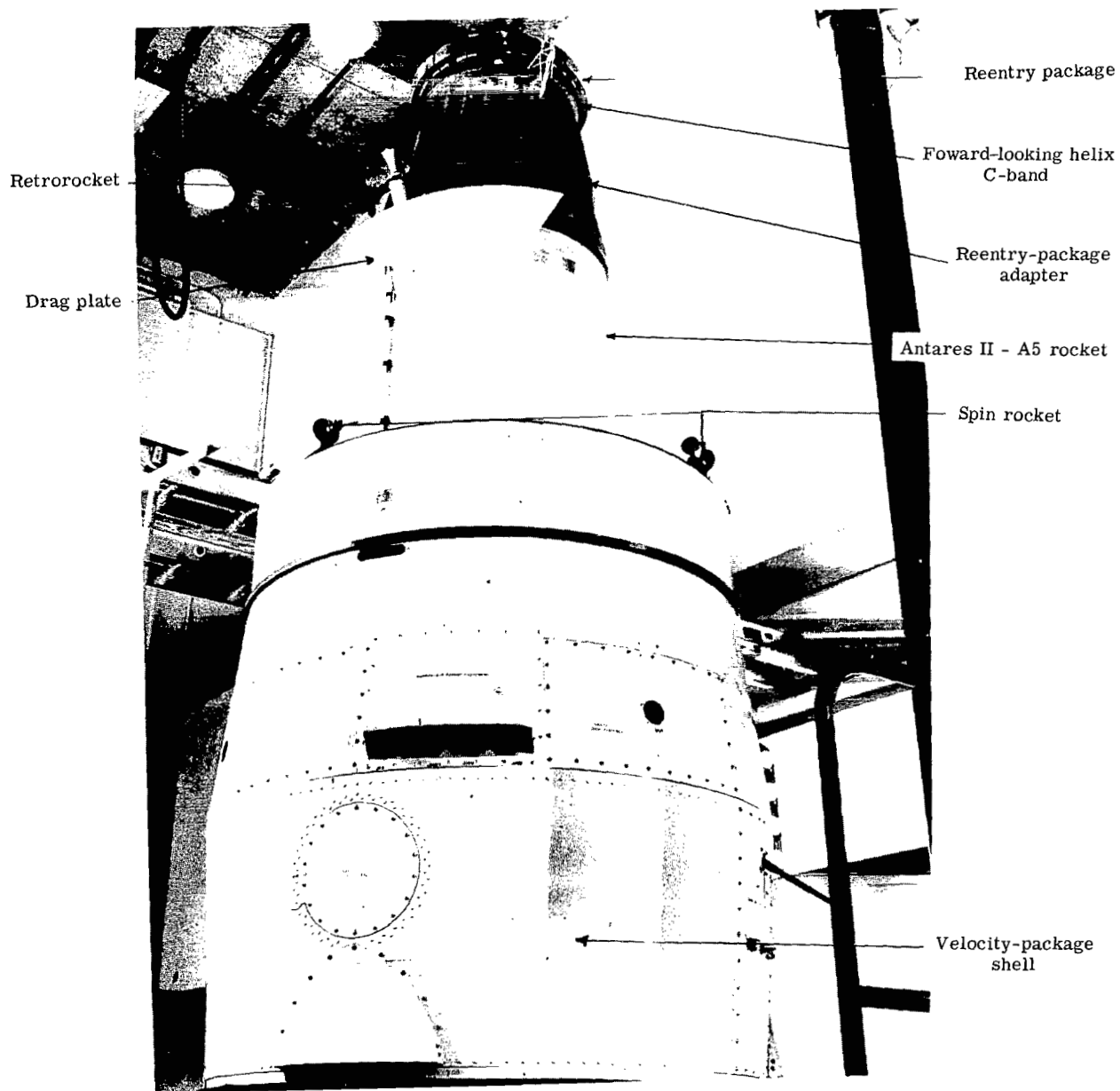
Figure 2.- Concluded.



Antares II - A5 rocket

Figure 3.- Fire II reentry-package adapter.

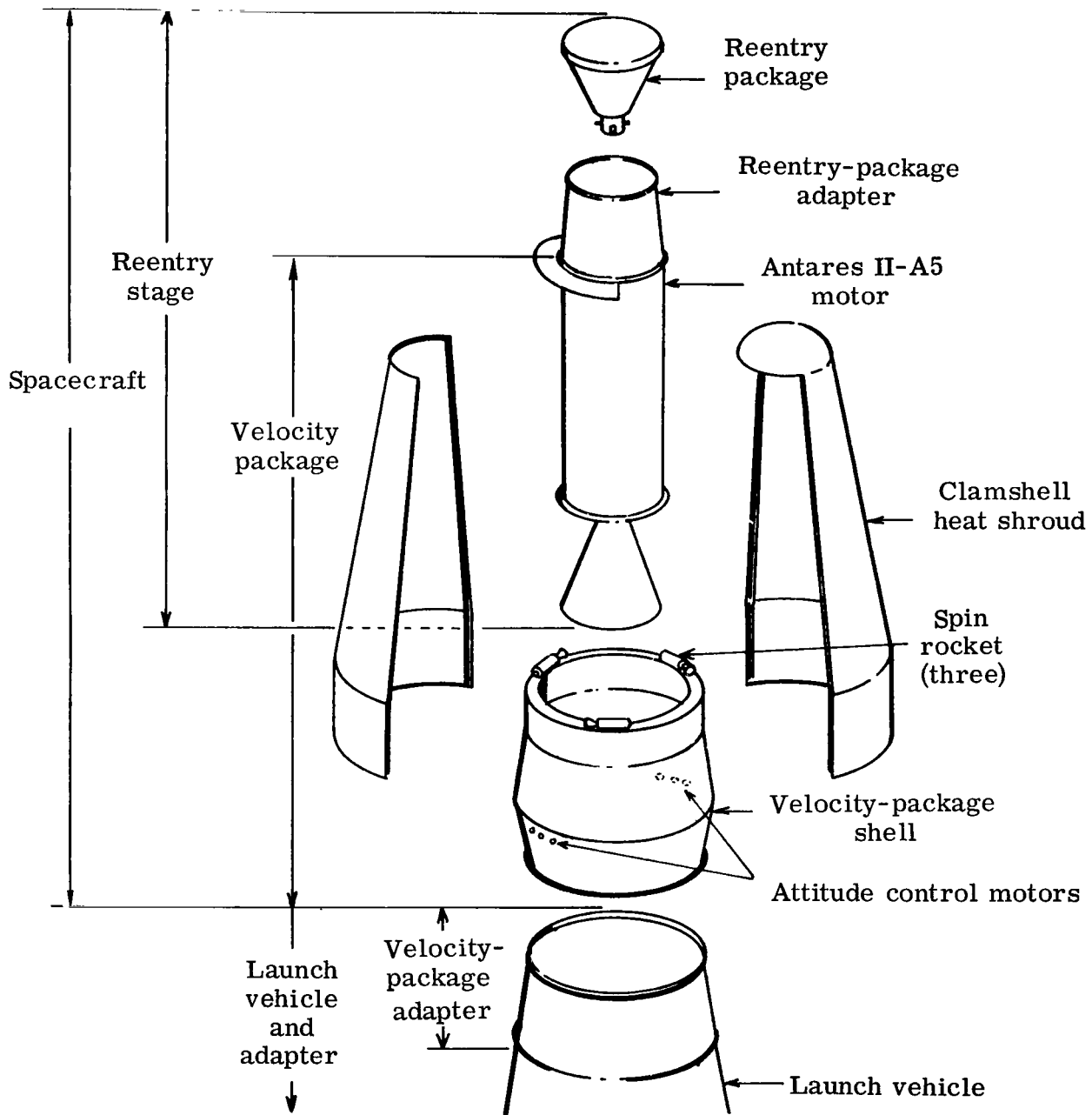
L-66-4444



(a) View with heat shroud removed.

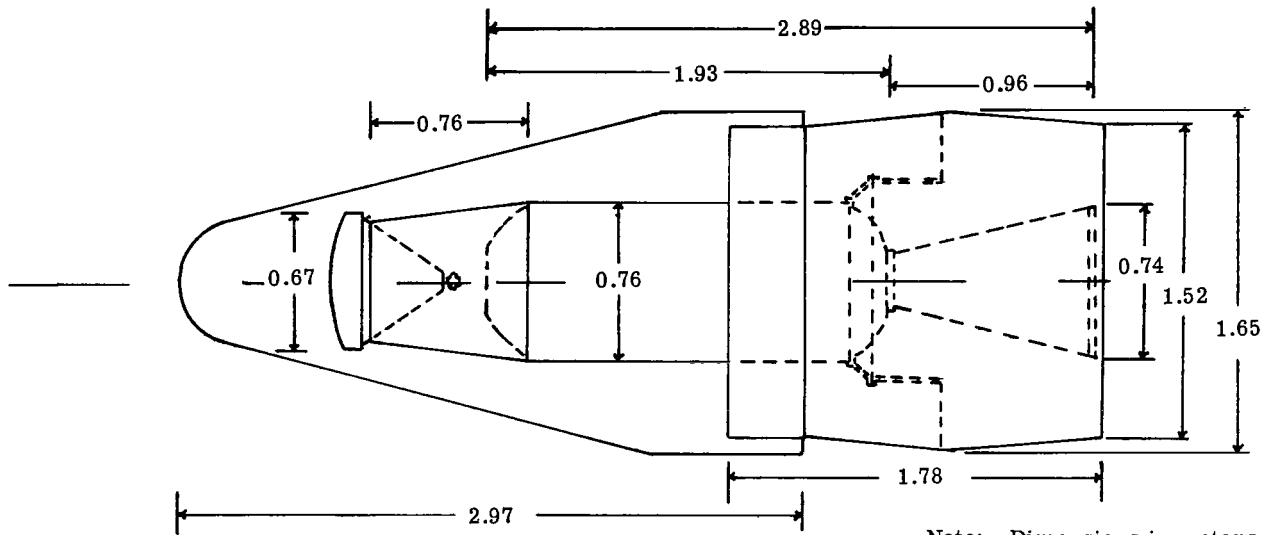
L-66-4445

Figure 4.- Fire II spacecraft.



(b) Exploded view.

Figure 4.- Continued.



Note: Dimensions in meters

Item	Weight, kg	Primary material	Item	Weight, kg	Primary material
Heat shroud (2 pieces)	133.66	Fiber glass Magnesium Aluminum	Spent Antares (which includes next three items)	143.73	Fiber glass Carbon
Reentry package	86.57 *	Beryllium Phenolic asbestos Aluminum	Reentry-package adapter	27.08	Fiber glass
Velocity-package shell	358.04	Aluminum	Drag plate + counterbalance	8.16	Aluminum Brass
			Motor adapter + balance mass	13.05	Aluminum Copper

\*0.454 kg of reentry-package coolant water not included.

(c) Physical characteristics.

Figure 4.- Concluded.

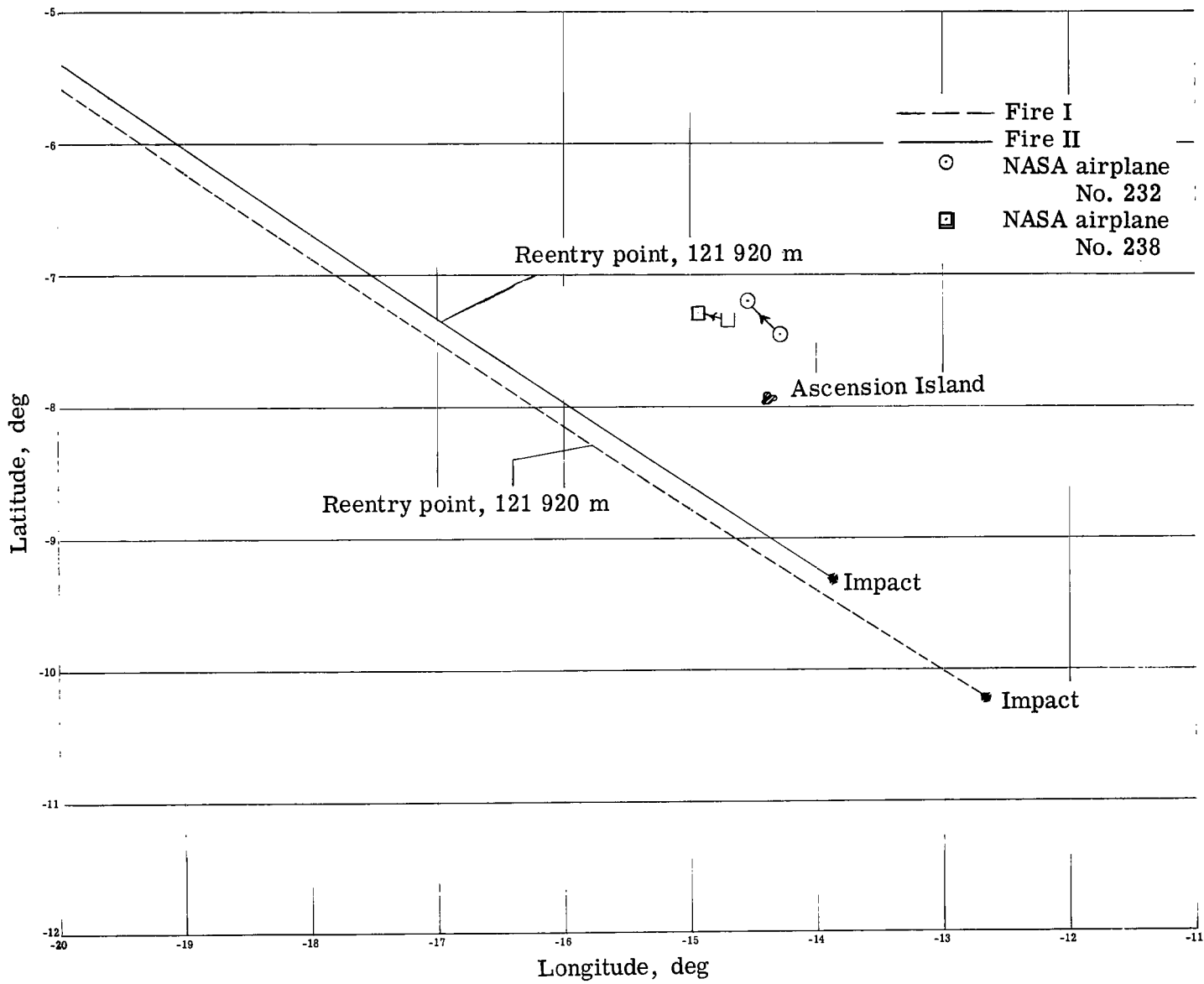


Figure 5.- Fire II reentry ground track.

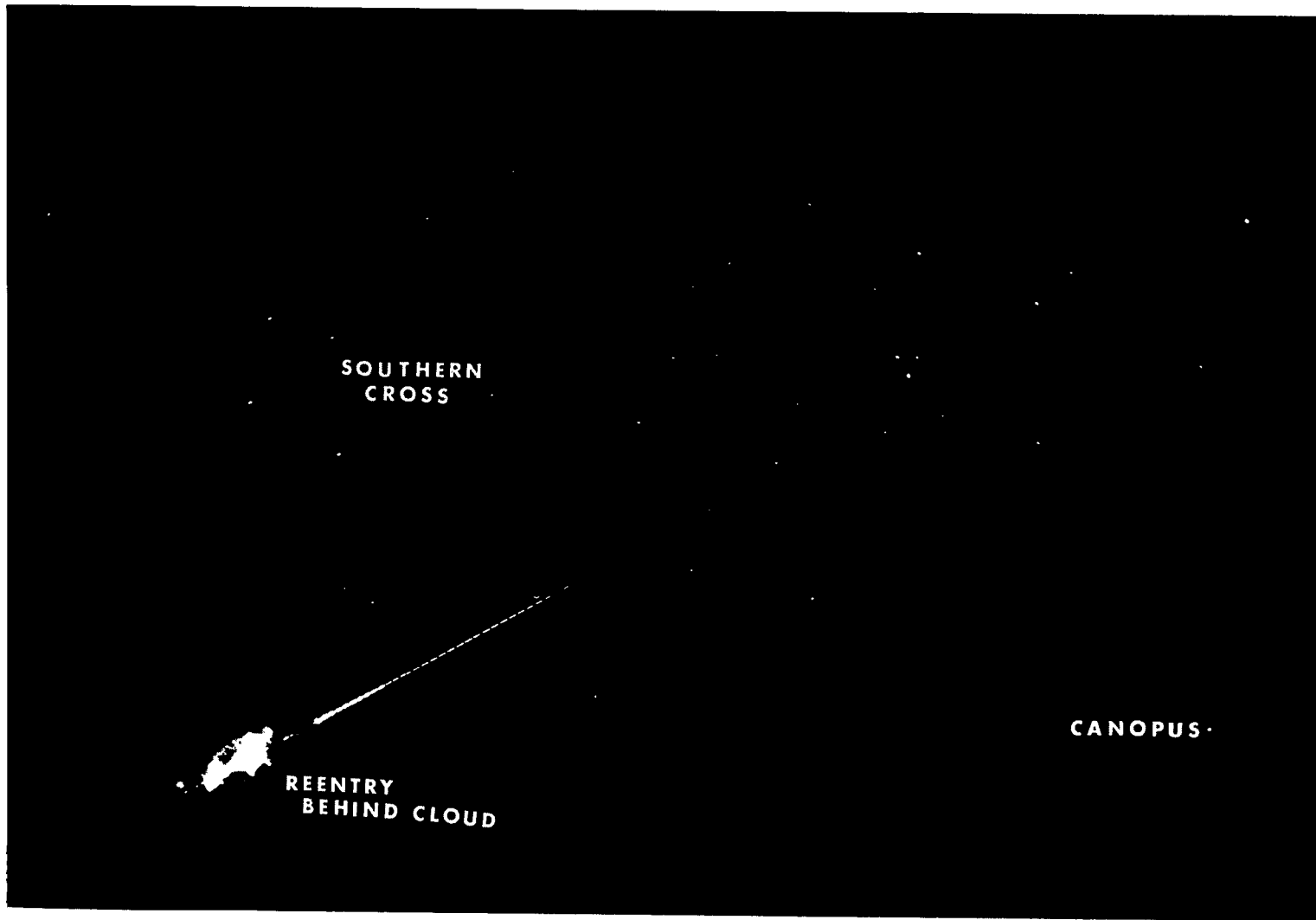


Figure 6.- Chopped photograph of Fire I reentry.

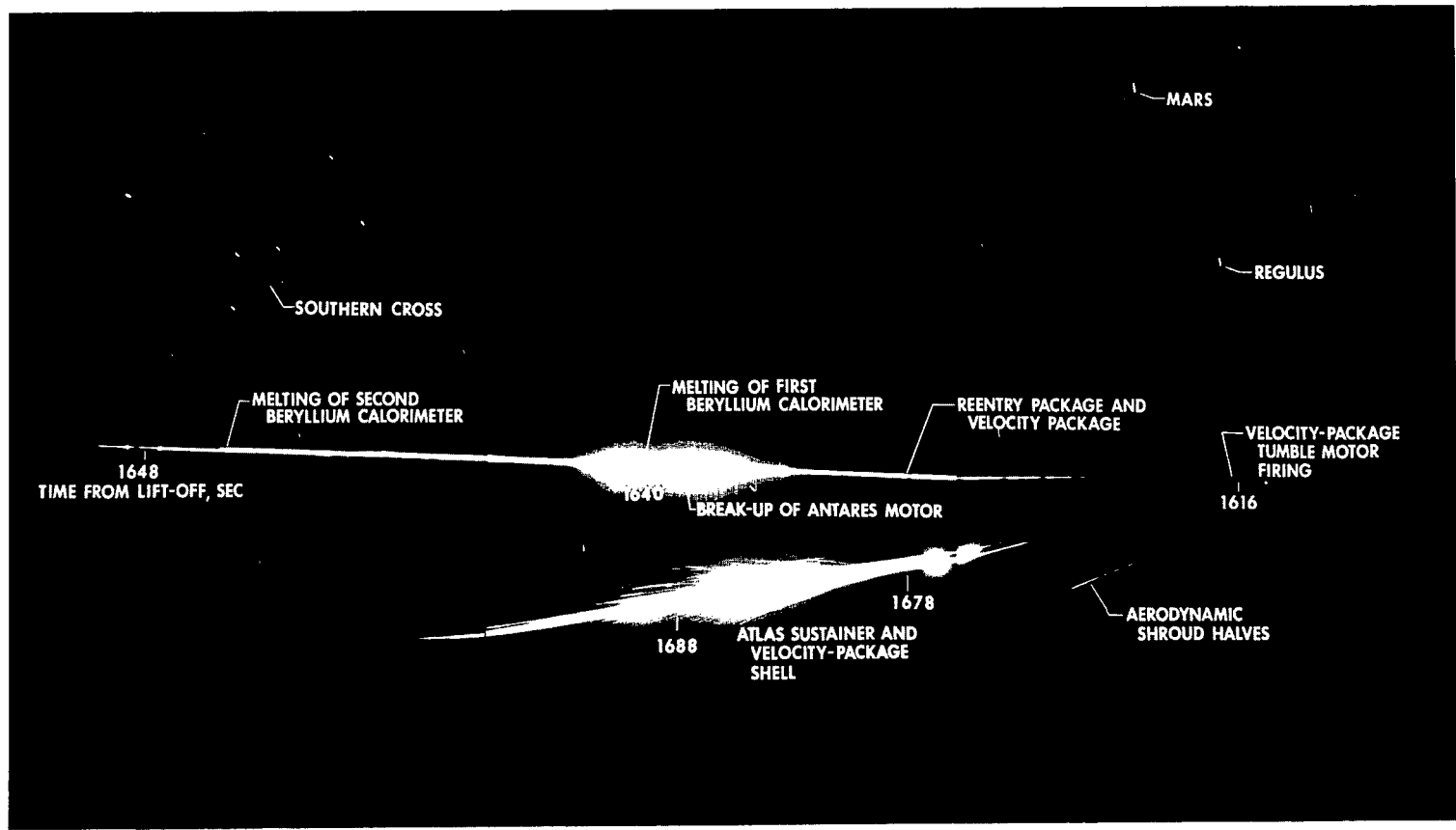


Figure 7.- Montage of Fire II reentry viewed from Ascension Island on May 22, 1965.

L-65-4713



RC-5 ballistic camera with a 152-millimeter focal length, an aperture of f/5.6, a vacuum-backed film magazine, and 038.01 high-speed panchromatic film. Shutter opened when airplane was positioned at latitude  $7^{\circ} 18' 30''$  S and longitude  $14^{\circ} 46' 30''$  W; shutter closed when airplane was at latitude  $7^{\circ} 18' 00''$  S and longitude  $14^{\circ} 50' 30''$  W.

Figure 8.- Open-shutter photograph of Fire II reentry taken from NASA airplane No. 238 at an altitude of 3200 meters and a heading of  $292^{\circ}$  when the shutter opened and  $277^{\circ}$  when the shutter closed.

L-66-4446

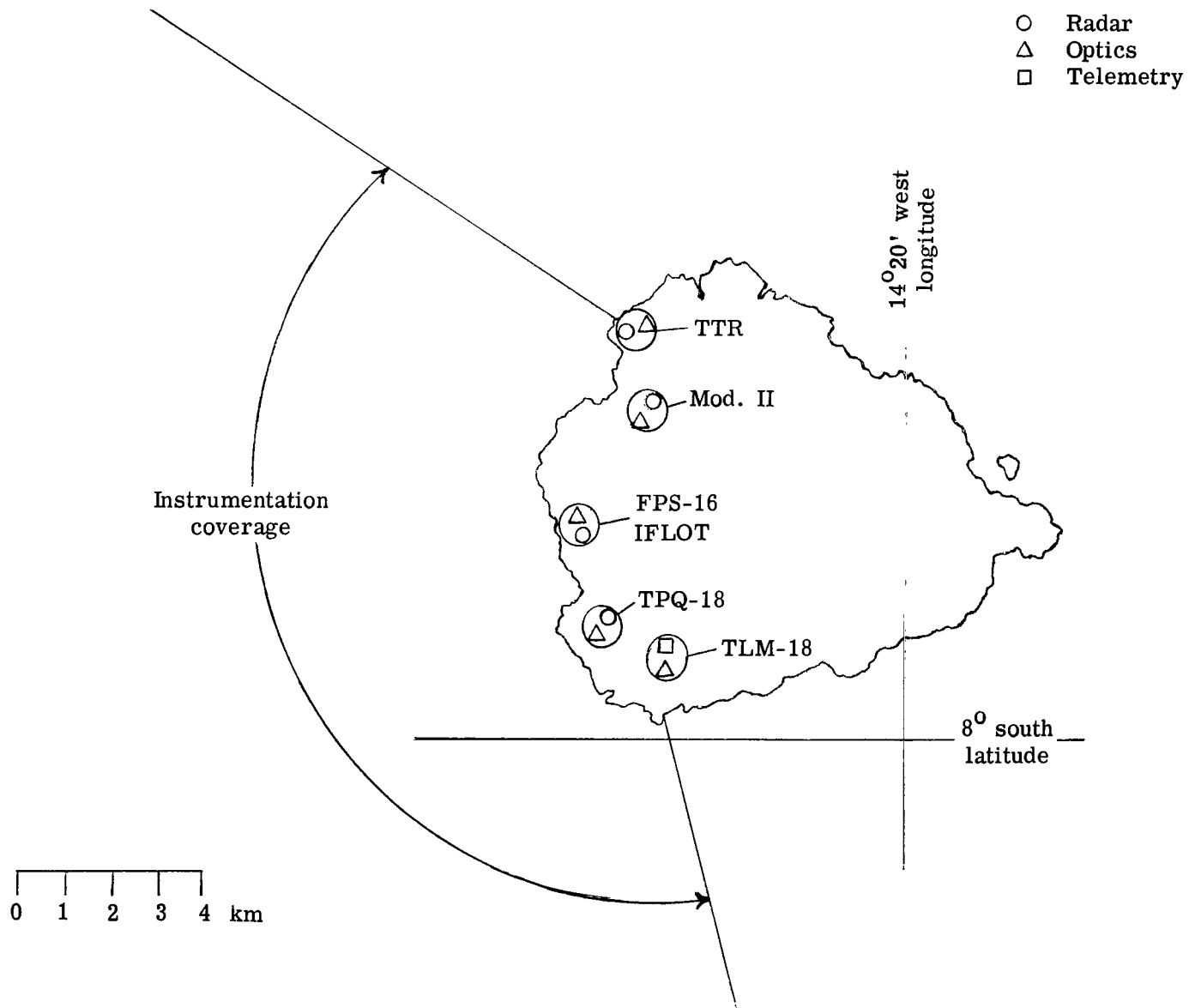
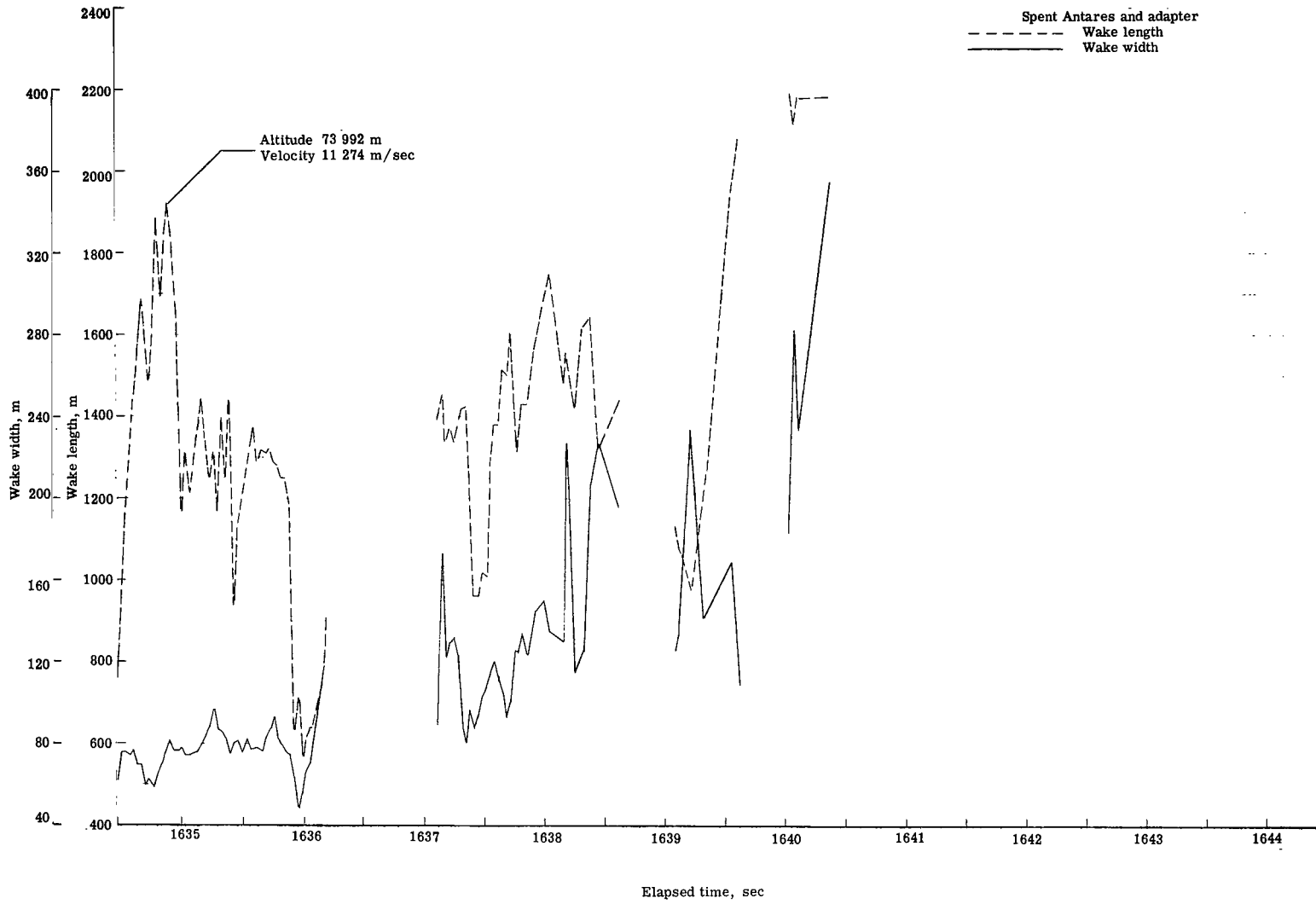
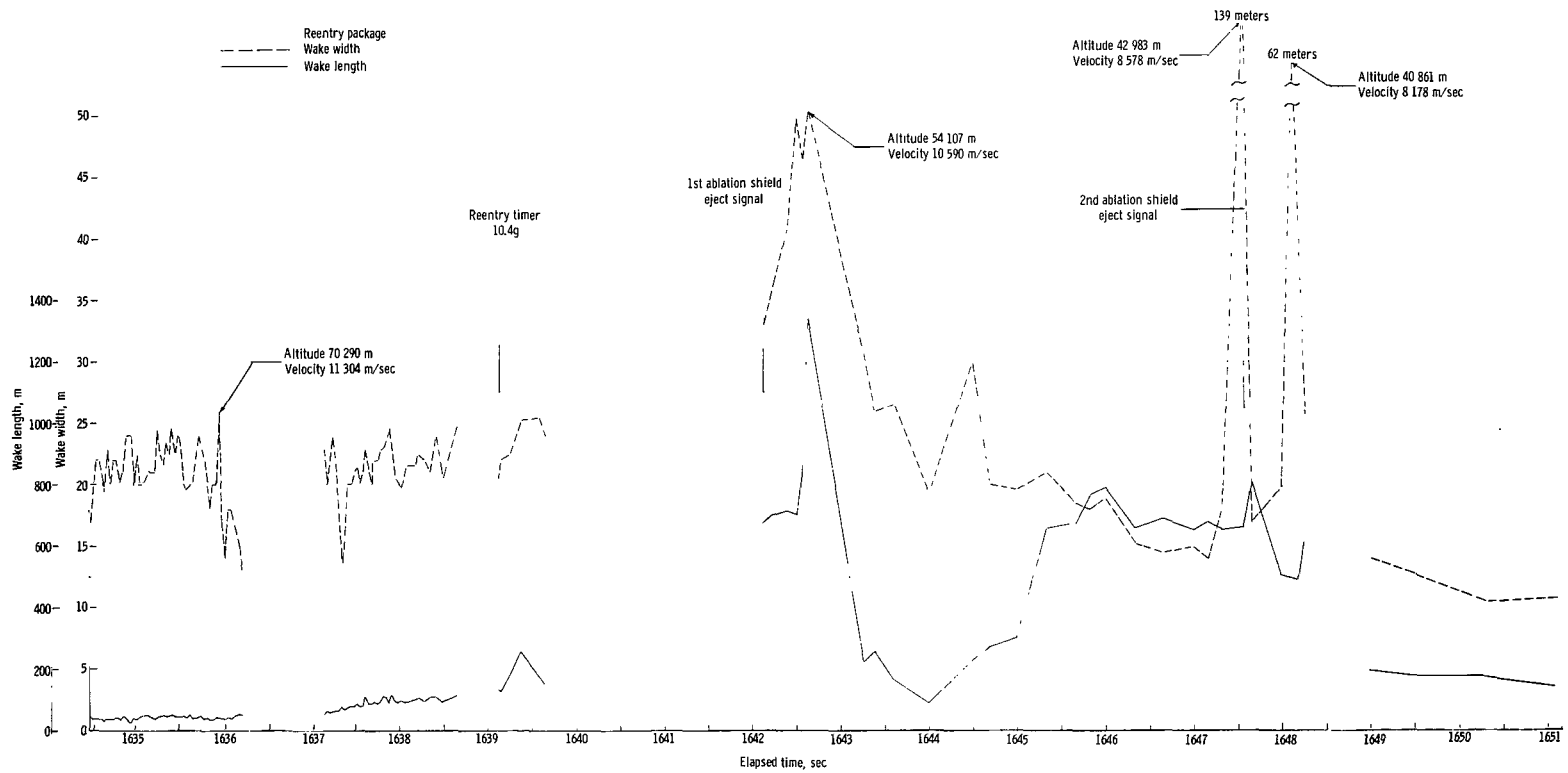


Figure 9.- Ascension Island instrumentation deployment.



(a) Spent velocity package.

Figure 10.- Visible wake dimensions.



(b) Reentry package.

Figure 10.- Concluded.

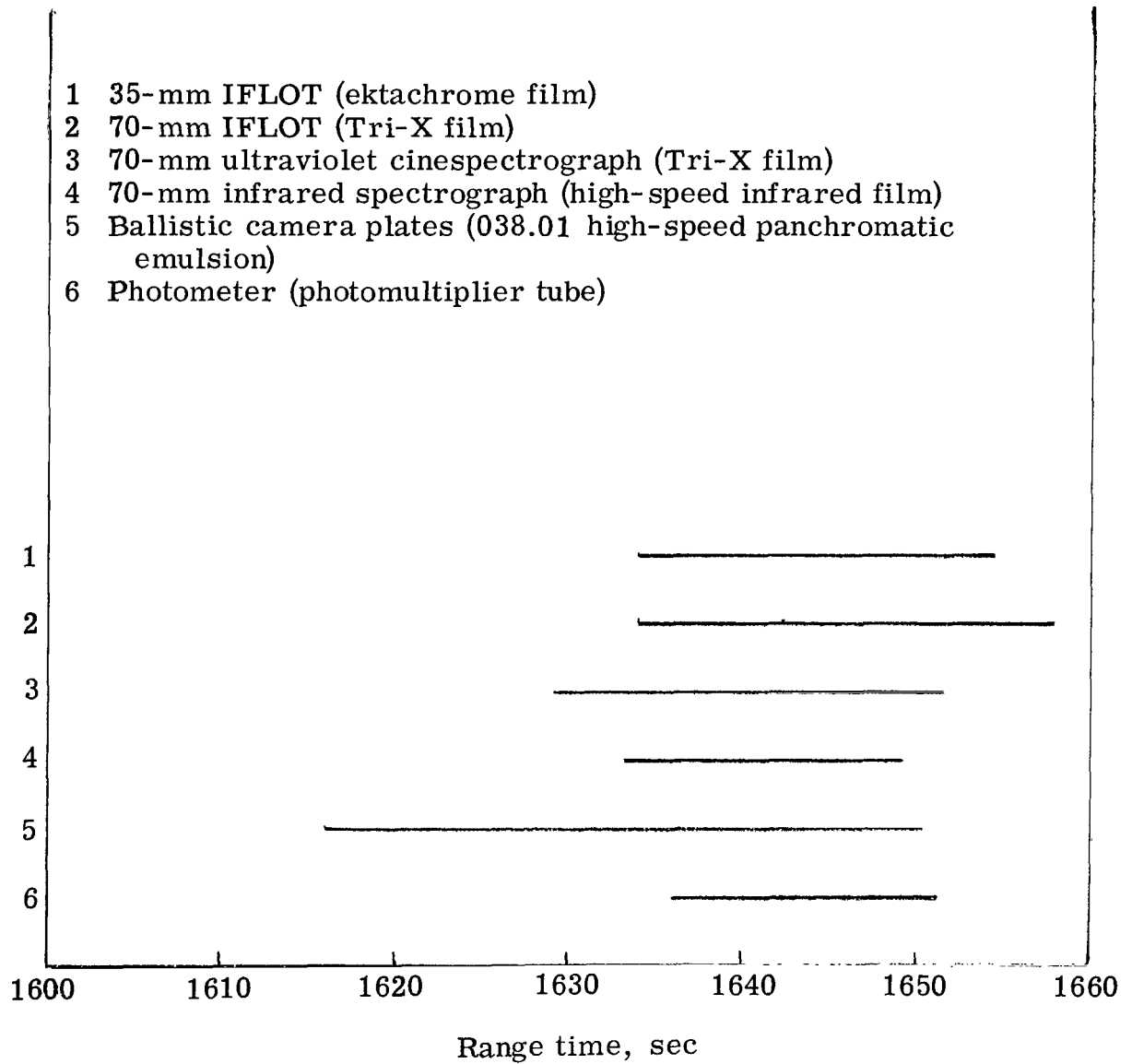
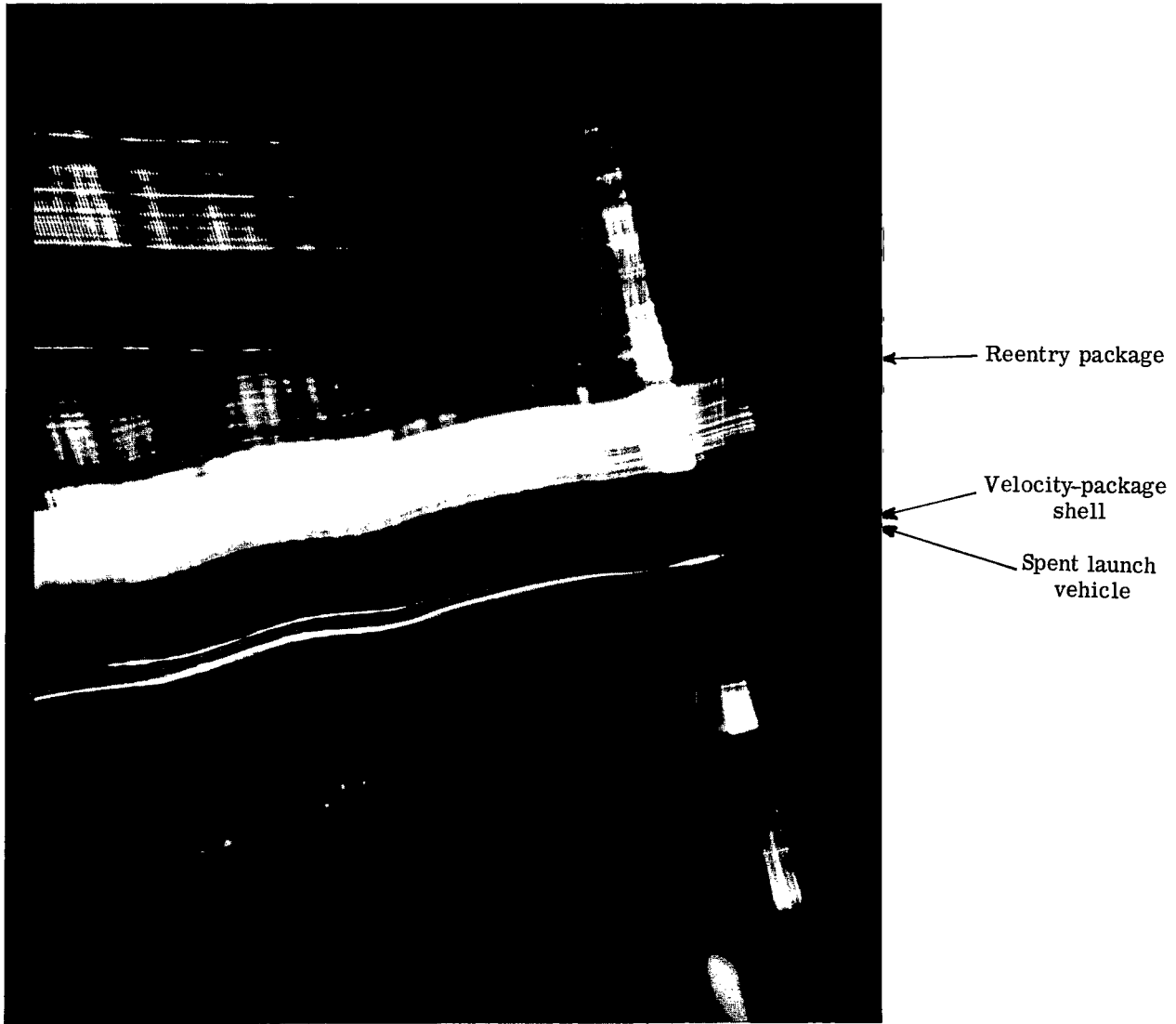


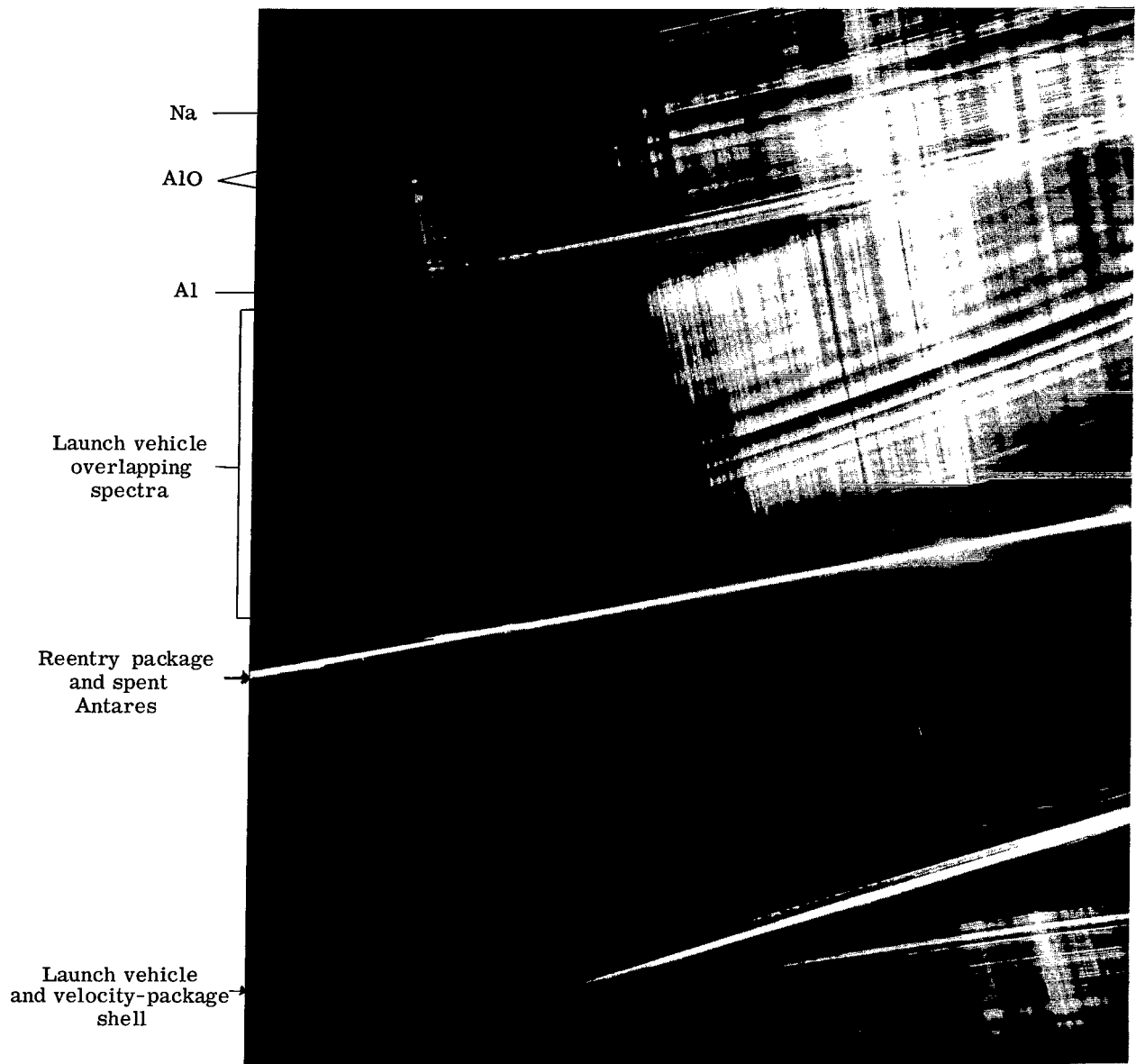
Figure 11.- Instrumentation and coverage times for signature data reduced by Eastern Test Range (ref. 3).



(a) Spectrograph made from NASA airplane No. 238. K-37 camera; 150 lines/mm.

L-66-4447

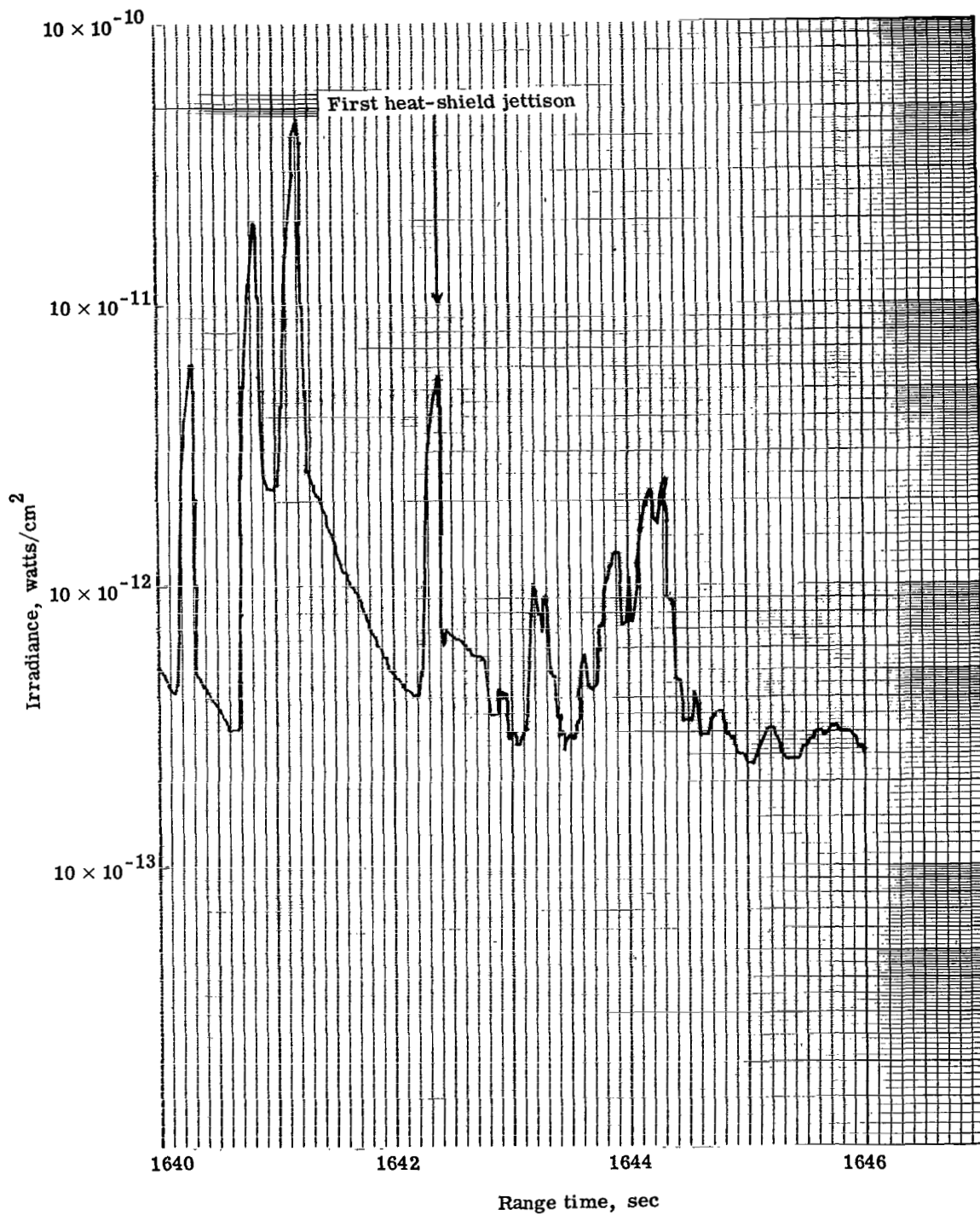
Figure 12.- Ballistic spectrographs.



(b) Spectrograph made from Ascension Island. K-37 camera; 600 lines/mm.

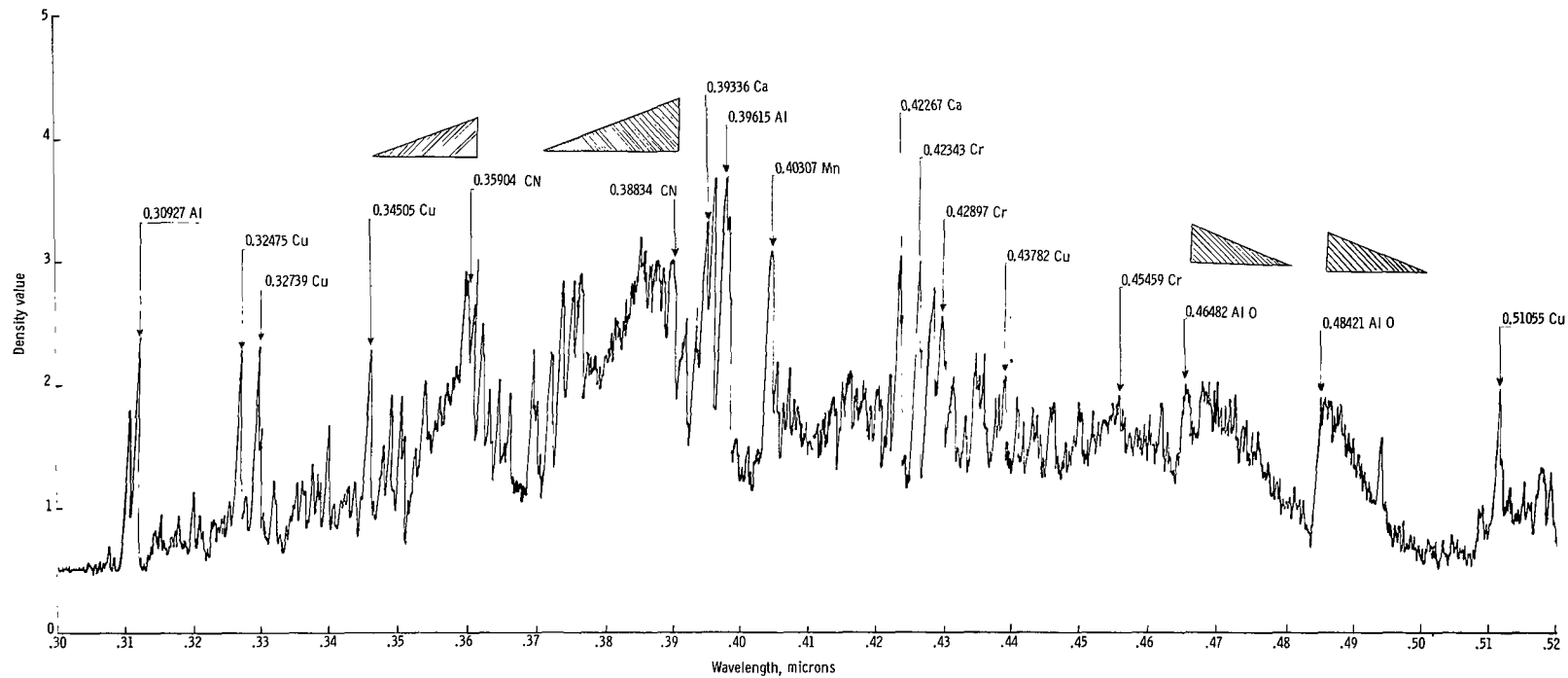
L-66-4448

Figure 12.- Concluded.



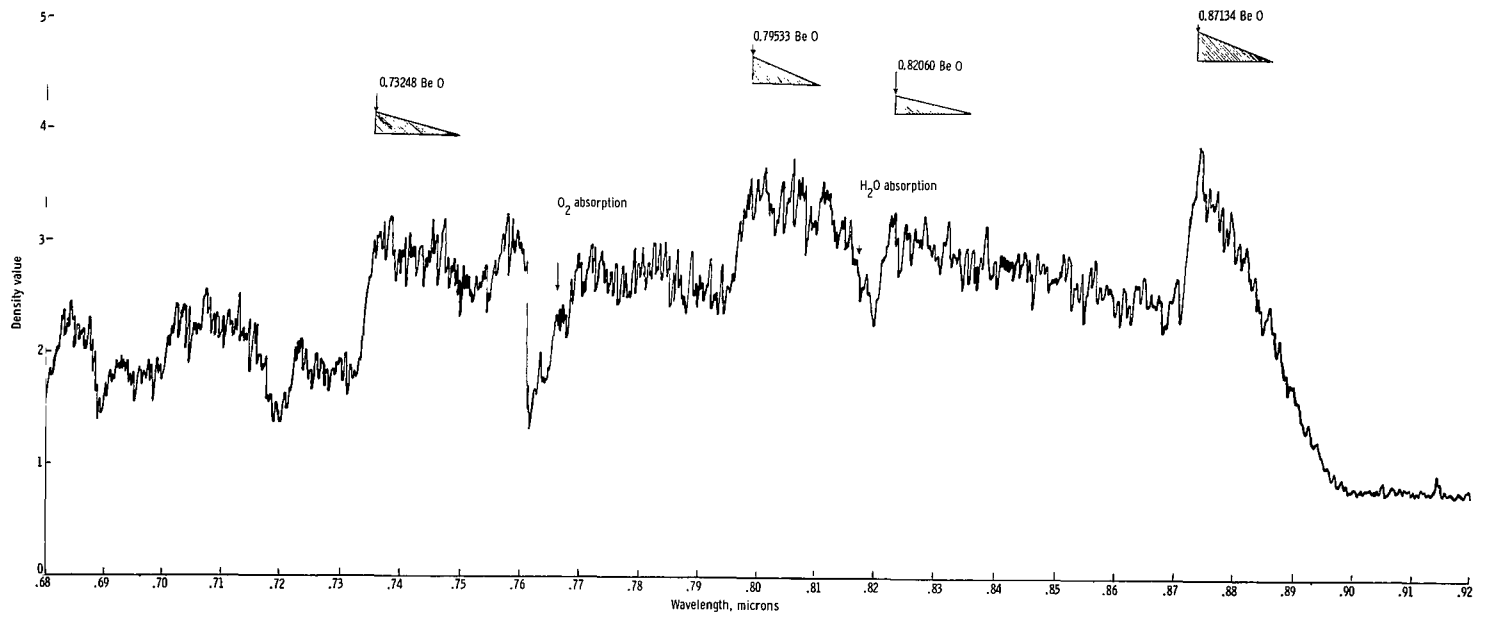
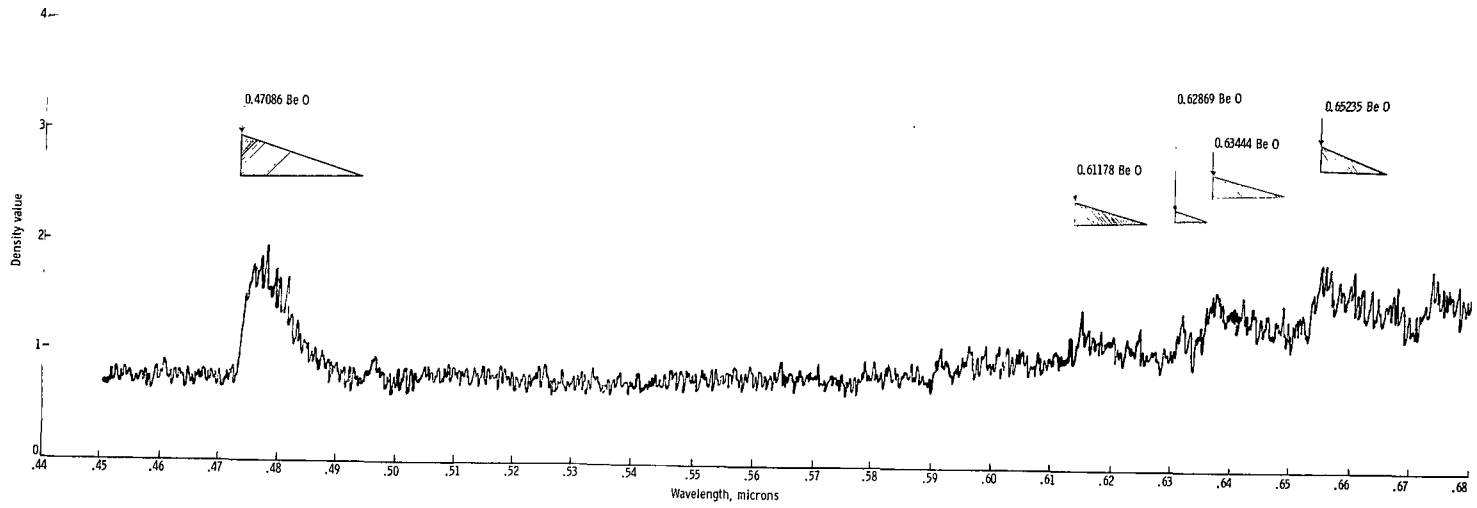
(a) Irradiance as a function of time, measured at 0.42 micron.

Figure 13.- Optical signature reduction.



(b) Density as a function of wavelength (ultraviolet-visible).

Figure 13.- Continued.



(c) Density as a function of wavelength (infrared-visible).

Figure 13.- Concluded.

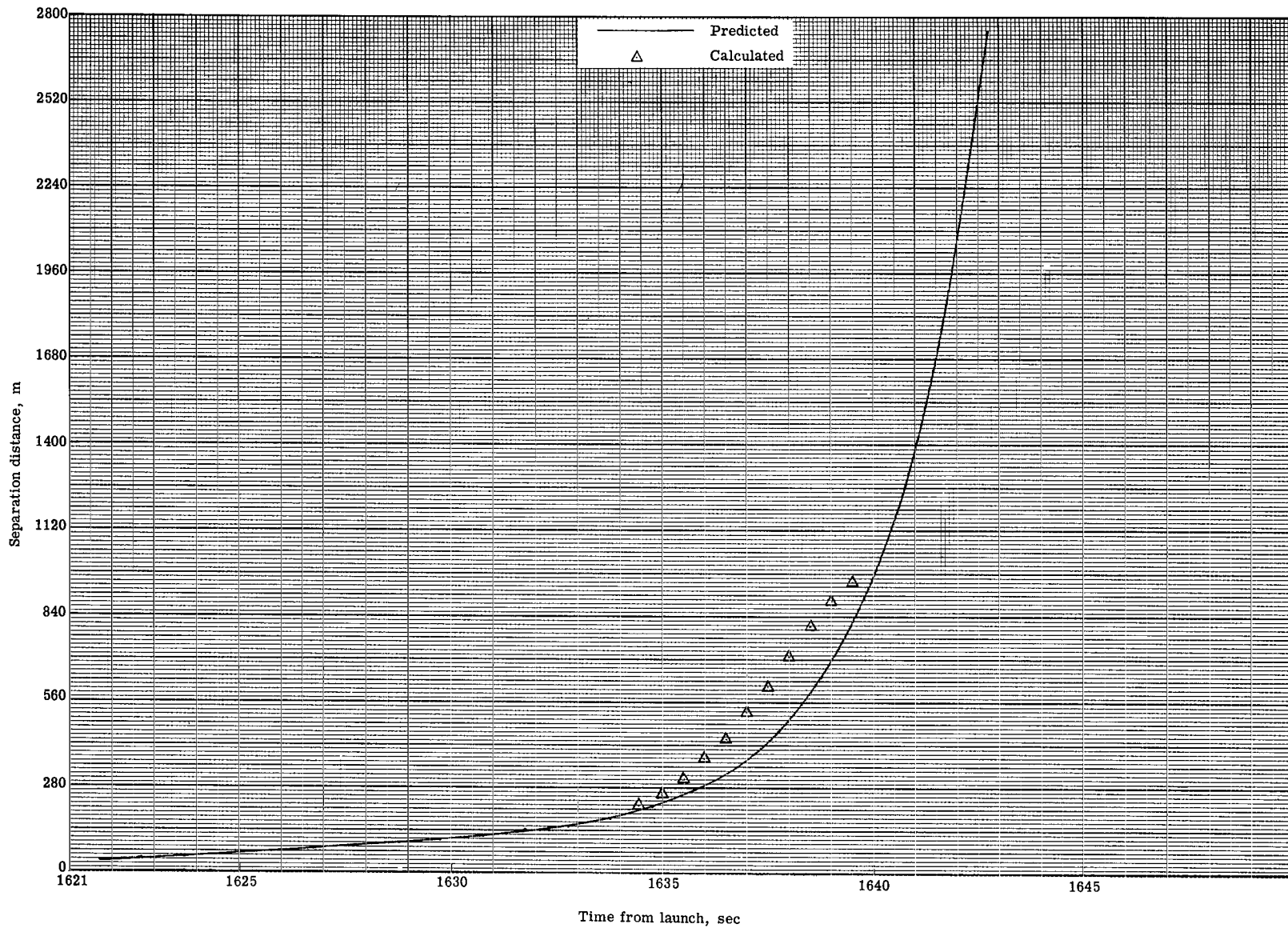


Figure 14.- Separation distance between Fire II reentry package and nearest component of the spent Antares and adapter.

*"The aeronautical and space activities of the United States shall be conducted so as to contribute . . . to the expansion of human knowledge of phenomena in the atmosphere and space. The Administration shall provide for the widest practicable and appropriate dissemination of information concerning its activities and the results thereof."*

—NATIONAL AERONAUTICS AND SPACE ACT OF 1958

## NASA SCIENTIFIC AND TECHNICAL PUBLICATIONS

**TECHNICAL REPORTS:** Scientific and technical information considered important, complete, and a lasting contribution to existing knowledge.

**TECHNICAL NOTES:** Information less broad in scope but nevertheless of importance as a contribution to existing knowledge.

**TECHNICAL MEMORANDUMS:** Information receiving limited distribution because of preliminary data, security classification, or other reasons.

**CONTRACTOR REPORTS:** Technical information generated in connection with a NASA contract or grant and released under NASA auspices.

**TECHNICAL TRANSLATIONS:** Information published in a foreign language considered to merit NASA distribution in English.

**TECHNICAL REPRINTS:** Information derived from NASA activities and initially published in the form of journal articles.

**SPECIAL PUBLICATIONS:** Information derived from or of value to NASA activities but not necessarily reporting the results of individual NASA-programmed scientific efforts. Publications include conference proceedings, monographs, data compilations, handbooks, sourcebooks, and special bibliographies.

*Details on the availability of these publications may be obtained from:*

SCIENTIFIC AND TECHNICAL INFORMATION DIVISION  
NATIONAL AERONAUTICS AND SPACE ADMINISTRATION  
Washington, D.C. 20546